Journal Pre-proofs

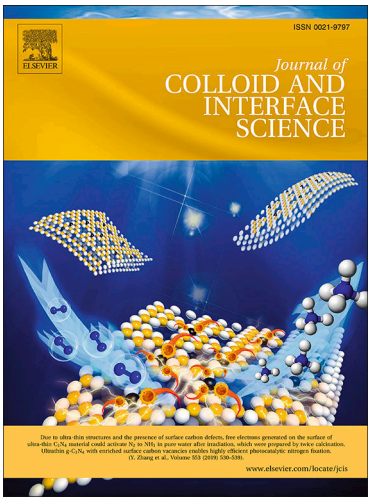

An adhesive and injectable nanocomposite hydrogel of thiolated gelatin/ gelatin methacrylate /Laponite® as a potential surgical sealant

Negar Rajabi, Mahshid Kharaziha, Rahmatollah Emadi, Ali Zarrabi, Hamidreza Mokhtari, Sahar Salehi

PII: S0021-9797(19)31507-3
DOI: https://doi.org/10.1016/j.jcis.2019.12.048
Reference: YJCIS 25788

To appear in: *Journal of Colloid and Interface Science*

Received Date: 28 September 2019
Revised Date: 12 December 2019
Accepted Date: 13 December 2019

Please cite this article as: N. Rajabi, M. Kharaziha, R. Emadi, A. Zarrabi, H. Mokhtari, S. Salehi, An adhesive and injectable nanocomposite hydrogel of thiolated gelatin/ gelatin methacrylate /Laponite® as a potential surgical sealant, *Journal of Colloid and Interface Science* (2019), doi: https://doi.org/10.1016/j.jcis.2019.12.048

An adhesive and injectable nanocomposite hydrogel of thiolated gelatin/ gelatin methacrylate /Laponite® as a potential surgical sealant

Negar Rajabi[1], Mahshid Kharaziha[1*], Rahmatollah Emadi[1], Ali Zarrabi[2], Hamidreza Mokhtari[1], Sahar Salehi[3]

1. Department of Materials Engineering, Isfahan University of Technology, Isfahan 84156-83111, Iran
2. Sabanci University Nanotechnology Research and Application Center (SUNUM), Orta Mah., Tuzla 34956, Istanbul, Turkey
3. Department of Biomaterials, University of Bayreuth, Bayreuth 95447, Germany

*Corresponding author E-mail address: kharaziha@cc.iut.ac.ir

Abstract

Hemostatic adhesive hydrogels as sealants for surgical operations are one of the focus of the researches in the field of injectable materials. Herein, we evaluated the potential application of a mechanically robust nanocomposite hydrogel with significant adhesion strength and shorter blood clotting time. This hydrogel was composed of thiolated gelatin (Gel-SH) and gelatin methacrylate (GelMA) as the main matrix to support cell viability and proliferation, while polydopamine functionalized Laponite® (PD-LAP) were introduced to the structure to improve the mechanical properties, adhesion strength, and blood clotting. This hydrogel formed via Michael reaction between Gel-SH and GelMA, and covalent interaction between PD-LAP and hydrogel. Results revealed that presence of-PD-LAP significantly controlled the swelling ratio, biodegradability, and mechanical properties of nanocomposite hydrogels. Tensile and compressive strength of nanocomposite hydrogels were measured in the range of 22-84 kPa and 54-153 kPa, respectively. Furthermore, nanocomposite hydrogels revealed excellent recovery ability, strong tissue adhesiveness and significantly less blood clotting time than Gel-SH/GelMA hydrogel (2.25 min). In the culture with L929 fibroblasts cells, viability more than 97% and high proliferation after 5 days of culture was estimated. The simplicity, low-cost, tunable mechanical properties, short blood clotting time, and cytocompatibility of the hydrogels composed of Gel-SH, GelMA, and PD-LAP highlight its potential as hemostat sealants.

Keywords: Thiol-methacrylate chemistry; Methacrylate gelatin; Thiolated gelatin; Visible photo crosslinking; Surgical sealants.

1. Introduction:

According to the World Health Organization (WHO) report, 356 million operations occurred in 2012, while they are anticipated to rise by 38% in 2020. Current surgical closure materials and techniques such as sutures, staples, wires, and clips have been widely used in different surgeries for a long time[1]. Despite their accessibility, ease of use and cheapness, they may result in air or fluid leakage, and microbial infection [2]. Moreover, the old surgical closure materials may increase the length and cost of hospitalization, while they are inappropriate for sensitive surgeries such as nerve, ocular, and vascular operations[3]. Recently, surgical gules have been recommended as alternatives for internal surgical closure materials, due to the relative ease of use and to prevent further damage. The internal surgical glues have to stimulate blood clotting, while acting as barriers against air and liquid leakage. Moreover, they should be biocompatible without causing any infection and side effects, and with controlled degradation rate under the physiological condition. Besides, the mechanical strength of surgery glues has to be adjustable depending on the type of the tissue[4]. Setting time, non-pyrogenic crosslinking, and proper swelling ratio are other important factors for selection of an optimized glue for a specific application[4]. Finally, tissue adhesives need to have robust wet adhesion [4].

Various types of synthetic and natural polymers and hydrogels have been applied as surgical glues[2, 4]. Between the natural polymers, gelatin derived from denaturation of collagen is one of the most available, biocompatible, biodegradable and non-immunogenic biopolymers [5]. However, in physiological conditions and due to the hydrolysis and *enzymatic* reactions, gelatin quickly degrades. Therefore, the mechanical strength and the hemostatic capability of gelatin adhesives are not adequate [6] [7]. One of the promising approaches to overcome these issues is copolymerization of gelatin with various functional groups and s*ynthesis* of modified structures such as gelatin methacrylate (GelMA), aminated (Gel-NH_2) and thiolated gelatin (Gel-SH). Nicolas et al.[8] proposed a modification approach based on disulfide crosslinking of collagen hydrogels. They produced a film by generating disulfide bindings which resulted in acceptable mechanical properties and high resistance against enzymatic degradation. However, thiolated collagen suffers from the water solubility. Moreover, crosslinking process of Gel-SH is very slow, making it not suitable for wound dressing and surgical sealants[9].

Another approach to control the gelation and degradation rate of disulfide-based crosslinking of hydrogels is Michael addition reaction, which is based on nucleophilic addition between Michael acceptors and donors[10, 11]. The hydrogels synthesized through this reaction can be cross-linked faster within a few minutes with improved stability in physiological condition [12]. In this regard, a Michael addition has been reported between Gel-SH [10], heparin [13], chitosan[14], hyaluronic acid [9] and other polymers such as

polyethylene glycol diacrylate (PEGDA). However, PEG, as a synthetic polymer lacks the suitable biofunctional groups which are necessary for cell interactions [12].

Hybrid hydrogels containing different types of additives such as graphene oxide[15], carbon nanotubes[16], metal and metal oxide nanoparticles [17], and nanoclays [18] have been introduced as an adhesive hydrogels with improved mechanical properties. Among the nanostructured reinforcements, from Smectite family, is Laponite®(LAP), $Na_{0.7}Si_8Mg_{5.5}Li_{0.3}O_{20}(OH)_4$, with disk-like structure and diameter of 20-30 nm [19]. There has been many reports on the application of LAP nanoplates in drug delivery [20], wound dressing [18] and bone tissue engineering [21, 22]. Moreover, due to the surface charge and particular disk-like structure, LAP has been known as an effective hemostatic agent [23]. Gaharwar et al. [7] developed a gelatin-LAP hydrogel and confirmed this hydrogel decreased the blood clotting time by 77%. Furthermore, incorporation of LAP nanoplates in the hydrogel improved its shear-thinning properties, making it suitable for hemorrhage usage [7]. Häffner et al. [24] reported the antibacterial effect of LAP nanoplates hindering initiation of infection and inflammation reaction in the wound. To increase the adhesion strength and uniform distribution of LAP nanoplates in any hydrogel-based materials, various surface modification approaches have been applied [25]. In this regard, mussel-inspired materials consisting of DOPA and polydopamine have been used by Han et al. [4] to modify the nanoclays in the composition of adhesive hydrogel with improved long-term mechanical stability as a wound dressing [4].

In this study, we introduced an adhesive hydrogel with hybrid structure based on gelatin laden polydopamine modified LAP (PD-LAP) and evaluated the role of PD-LAP and various concentrations of plate-like PD-LAP (0, 0.5, 1, 2 wt%) on the properties of hydrogels. Blended hydrogel comprising Gel-SH and GelMA has an advantage of multi-crosslinking system in gelatin, based on Thiol-methacrylate chemistry. It was anticipated that the incorporation of PD-LAP in the gelatin-based hydrogel could provide a cytocompatible hydrogel with suitable physical, mechanical and biological properties, and improved hemostasis behavior due to the presence of PD-LAP which can introduce the nanocomposite hydrogel as a surgical sealant.

2. Material and Method

2.1. Materials

Type A gelatin from porcine skin (300 bloom), 1-ethyl-3-[3-dimethylaminopropyl] carbodiimide hydrochloride (EDC), ethylenediamine (≥ 99.0%), 2-iminothiolane (≥98.0%), methacrylic anhydride (94%), triethanolamine (TEA, ≥99.0%), N-vinylcaprolactam (VC, 98%), Eosin Y (~99%), 5,5'-

Dithiobis(2-nitrobenzoic acid) (DTNB) (≥98.0%), L-Cysteine (≥97.0%) and sodium borohydride (≥98.0%) were purchased from Sigma-Aldrich. Synthetic silicate nanoplates (Laponite® RDS) composed of SiO_2 (60%), MgO (27%), Na_2O (3%) and Li_2O (1%) was bought from Rockwood Additives Limited, UK. Dopamine hydrochloride (DA, $C_8H_{11}NO_2$) was obtained from Merck Millipore. Dialysis membrane (molecular weight cutoffs (MWCO) of 12-14 kDa) was provided from Betagen Co, Mashhad, Iran. Moreover, deionized (DI) water was applied in all experiments.

2.2. Synthesize of thiolated gelatin (Gel-SH)

Following Duggan report with some changes [6], Gel-SH was firstly aminated, where one gram gelatin was dissolved in 25 ml of 0.1 M phosphate buffer (pH 5.1) at 40°C and stirred for 1 h. After complete dissolution and addition of ethylenediamine (3.14 ml), the pH value of the solution was adjusted to 5 using 1M HCl. Followed by the addition of EDC (0.5 g), the reaction completed during 24 h, at ambient temperature. After that, the solution was dialyzed using a 12-14 kDa dialysis membrane against DI water in a dark room for 4 days. Finally, the solution was freeze-dried and stored at 4°C.

For the second-step thiolation, a solution of Gel-NH_2 (200 mg) in DI water (20 ml) was prepared. Consequently, 2-fold molar excess of 2-iminothilane added to this solution at ambient temperature and the pH value was adjusted to 7 using 1 M NaOH solution. After stirring of the solution at ambient temperature for 20 min, its pH value was reduced to 5. Then, the solution was dialyzed in the dark against one mM HCl solution (for 1 day), 5 mM HCl (for 1 day), and another day against one mM HCl solution, subsequently. Lastly, the solution was freeze-dried and stored at 4°C for further experiments (two-step thiolation). To investigate the role of the amination process, a similar approach was performed on the primary gelatin (one-step thiolation).

2.3. Synthesize of gelatin methacrylate (GelMA)

GelMA, with a high methacrylation degree, was synthesized, according to Nichol et al.[26]. Briefly, 10 wt% gelatin solution in phosphate buffer saline (PBS, pH=7.4) at 40°C was prepared. PBS was prepared based on a previous protocol [27]. After complete dissolution, methacrylation reaction was started by adding 20 ml of methacrylic anhydride to the gelatin solution and it was stirred under 40°C for 2 h. To stop the methacrylation process, two-fold dilution of pre-warmed PBS (40°C) was used and final solution was dialyzed against distilled water for 7 days at 40°C to remove unreacted monomers and salts. The solution was finally freeze-dried for 2 days and kept at 4°C for further experiments.

2.4. Synthesize of polydopamine modified LAP nanoparticles

According to Con et al.[4] with some modifications, polydopamine modified LAP (PD-LAP) was prepared. Briefly, 0.057 wt% LAP nanoplates suspension in dopamine solution was prepared which was stirred for 5h at ambient temperature for intercalation and oxidation of dopamine. Finally, the suspension was freeze-dried to collect the PD-LAP powder.

2.5. Preparation of nanocomposite hydrogels

Primarily, 5 wt% GelMA solution in PBS at 60°C was prepared and mixed with PD-LAP at various concentrations including 0.5, 1 and 2 wt% until it was homogenously distributed. Then, 1.75 wt% of Gel-SH was added to the GelMA/PD-LAP solution and kept stirring at 40°C for 15 min. The ratio of Gel-SH and GelMA concentrations was selected based on the literature [28]. After 30 min mixing, 0.75 wt% TEA, as a co-initiator and 0.5 wt% VC as a co-monomer was added. In the next step, after 30 min stirring at room temperature, a mixture of this solution (10 µl) and 1 µl of 0.5 mM Eosin Y aqueous solution was prepared which could be cross-linked under various exposure time under blue-green light (100 Mw/cm^2) with wavelength in the range of 450-550 nm. Giving the concentration of PD-LAP (0.5, 1 and 2 wt%), the hydrogels were named Gel-0%PD-LAP, Gel-0.5%PD-LAP, Gel-1%PD-LAP and Gel-2%PD-LAP, respectively.

2.6. Characterization of nanocomposite hydrogels

The microstructure of the hydrogels was studied using scanning electron microscopy (SEM, Philips, XL30, Netherlands). Before imaging, the samples were frozen in liquid nitrogen, consequently lyophilized overnight and gold-coated using a sputter coater. After imaging of the hydrogel cross-section, at least 3 images from 3 individual samples, was used to measure the pore size of hydrogels using ImageJ. The modified LAP nanoplates were analyzed using a field emission-SEM (FE-SEM, QUANTA FEG 450, USA), X-ray diffraction (XRD, Phillips, Netherlands) and Fourier transform infrared spectroscopy (FTIR, Tensor27, Germany). Surface charge of the nanoplates of LAP and PD-LAP was measured in DI water at 25 °C using a 633nm laser Malvern ZEN3600 (Malvern Instruments, UK). Chemically modified hydrogels (Gel-NH_2, Gel-SH and GelMA) were also analyzed by FTIR and ^{1}H-NMR spectroscopy (Bruker Avance II, 500 MHz, Germany). ^{1}H-NMR spectra of gelatin, Gel-NH_2 and Gel-SH were performed in D2O at the frequency of 500 MHz. The amounts of free thiol groups were quantified photo-metrically, according to Ellman's reagent [6]. Briefly, the Gel-SH was dissolved in DI water with a concentration of 1 mg/ml and reduced with 0.1 M $NaBH_4$. Subsequently, Ellman's reagent (with the concentration of 4 mg/ml) was prepared in 0.1 M phosphate buffer at pH 8 and added to the above solution. After 2h incubation at room temperature in the dark, the absorbance of solutions was analyzed using a UV-Vis spectrophotometer at 412 nm. The

experiment was performed in triplicate. To determine the free thiol group content in gelatin, a curve of standard calibration by L-Cysteine was provided similarly.

2.7. Physiological stability assessment of nanocomposite hydrogels

To study the effect of PD-LAP concentration on the swelling ratio of nanocomposite hydrogels, the samples (n=3) were freeze-dried, weighed (W_1) and immersed in PBS solution (pH=7.4) for 24 h at 37°C. After 24 h incubation, the samples were weighed (W_2) and swelling ratio was measured, based on equations 1 [29]:

$$\text{Swelling ratio (\%)} = \frac{W2-w1}{W1} \times 100 \quad (1)$$

To evaluate the degradation rate, the nanocomposite hydrogels (n=3) were lyophilized and weighed (W_1), followed by immersing in PBS (pH=7.4) at 37°C. After 3, 7 and 14 days of incubation, the samples were lyophilized, weighted (W_2) and the weight loss of hydrogels was determined based on equation 2 [30]:

$$\text{Weight loss (\%)} = \frac{(W1-W2)}{W1} \times 100 \quad (2)$$

2.8. Mechanical properties of nanocomposite hydrogels

The mechanical properties (tensile, compression, and cyclic compression) of hydrogels containing various concentrations of PD-LAP were determined. Tensile properties of hydrogels were investigated using a tensile tester (Hounsfield H25KS, UK) with a load cell capacity of 500 N. The samples (n=3) with the dimension of 15mm×5mm×1mm were fixed between two tension grips and extended at the tensile rate of 1 mm/min until failure. The tensile test was also carried out to determine the elastic modulus, elongation, and toughness of samples. The elastic modulus determined from the slope of stress-strain curves in the linear region (0.05-0.15 strain).

The uniaxial compression test also performed on the cylindrical samples (n=3) with a diameter of 11 mm and a thickness of 3 mm at the strain rate of 1 mm/min. Consequently, the compressive strength was estimated from the stress-strain curves at 60% strain. Finally, to estimate the recovery ability of the samples (n=3), five compression recovery cycles, up to 40% strain at the loading rate of 0.5 mm/min, were carried out.

2.9. Adhesive strength of nanocomposite hydrogels

Tissue adhesive strength of samples was investigated according to ASTM F2458-05 standard, using a fresh sheepskin. At first, the sheepskin was incubated in PBS for 8 h to prevent drying during the experiment.

Then, the skin was fixed to the Ti sheet using glue, and 250 µl of each sample was applied on the 10 mm×15 mm of the sheepskin and crosslinked. The adhesive strength of samples was measured at the point of tearing at the strain rate of 10 mm/min.

2.10. Protein adsorption of nanocomposite hydrogels

Adsorption of bovine serum albumin (BSA) by composites was determined according to the batch contact method [31]. Briefly, after incubating in PBS for 3h, the samples (n=3) were weighted and immersed in 0.2 wt% BSA solution at room temperature for 30 min, while shaken slowly. Subsequently, the BSA absorption of the residual solution estimated using UV-vis spectrophotometer at 280 nm. Finally, the adsorbed BSA on the surface of samples determined according to equation 3 [18]:

$$\text{Adsorbed BSA} = \frac{(C0-Ca)}{W} \times V \quad (3)$$

In which C_0 and C_a are the concentration of BSA, before and after adsorption (mg/ml) on the hydrogel surface, respectively. Moreover, W and V are the weight of swollen samples (g) and the volume of BSA solution, respectively.

2.11. In vitro blood coagulation activity of nanocomposite hydrogels

Blood provided from an adult volunteer used in blood coagulation and hemocompatibility test of nanocomposite hydrogels. Blood collection performed based on the Iran national code of ethics for blood donation and transfusion. The blood was mixed with 3.8 wt% sodium citrate anticoagulant agent and diluted with normal saline in a volume ratio of 4:5. To investigate the blood coagulation activity of nanocomposite hydrogels, blood was primarily diluted in 0.024 ml of 0.2 mol/l $CaCl_2$ solution. Then, 0.27 ml of the diluted blood was added on the hydrogels and consequently was incubated at 37°C for 10 min. After that, 10 ml of DI water were added gradually and the sample solutions were centrifuged at 100×g for 30 s. Solutions were consequently diluted by DI water and kept at 37°C for 60 min. Subsequently, the absorbance of diluted samples was measured at 542 nm. Finally, the blood clotting time of samples was estimated by the BCI index, according to equation 4 [32]:

$$\text{BCI index} = \frac{100\times(abs\ of\ samples\ at\ 542\ nm)}{abs\ of\ ACD\ whole\ blood\ in\ water\ at\ 542\ nm} \quad (4)$$

Blood compatibility of samples was also investigated using Hemolysis ratio (HR) measurement. The samples with same size and containing different amounts of PD-LAP, at first, were rinsed with normal saline and water, and then, were soaked in 10 ml of normal saline at 37°C for 1h, under slight shaking. In the next step, samples were soaked in 0.2 ml diluted blood and supernatants were centrifuged at 100×g for

5 min. The positive and negative controls were 0.2 ml of diluted blood+10 ml water and 10 ml of normal saline, respectively. To estimate the HR of samples, the absorbance of supernatants was determined at 542 nm by UV spectroscopy. Finally, the HR was calculated, according to equation 5 [32]:

$$\mathrm{HR} = 100 \times \frac{(sample\ absorbance - negative\ control\ absorbance)}{(positive\ control\ absorbance - negetive\ control\ absorbance)} \quad (5)$$

2.12. In vitro cytocompatibility of nanocomposite hydrogels

L929 fibroblasts cells, purchased from Royan Institute of Iran, were used to study the cytocompatibility of nanocomposite hydrogels. The disk-shape samples with 3 mm thickness were prepared, rinsed with PBS (Bioidea) and sterilized under UV for one hour. The cells with a density of 10^4 cells/ml were subsequently cultivated on the hydrogels and control tissue culture plate (TCP, control) for 1, 3 and 5 days. The culture medium contains Dulbecco's Modified Eagle Medium (DMEM, Gibco), 10%(v/v) Fetal bovine serum (Gibco) and 1%(v/v) streptomycin/penicillin (Gibco). The metabolic activity of cells was measured via MTT assay, based on manufacture protocol (Sigma, USA). At the specific time points (1, 3 and 5 days), the cell-seeded samples were incubated with MTT solution (0.5 mg/ml) for 4 h at 37°C. Then, the formed formazan crystals were dissolved in DMSO. The optical density (OD) of samples was determined using a microplate reader (Biotek Instruments) at 570 nm. Finally, the relative cell survival (% control) was determined using equation 6:

$$\text{Relative cell survival (\%control)} = \frac{(X\ sample - Xb)}{(Xc - Xb)} \quad (6)$$

Where XSample, Xb and Xc are the absorbance of samples, DMSO, and control (TCP), respectively.

To study the effects of hydrogel composition on the cell viability, live/dead assay (Biotium, UK) was performed, according to manufacturer's protocol. After 1 and 3 days of culture, the cell-seeded samples (n=3) were stained with dilution of 4 µM ethidium homodimer-1(EthD-1) and 2µM calcine AM in PBS. After 20 min incubation at 37°C, the samples were rinsed with PBS and consequently, were imaged using a fluorescence microscope (Nikon TE 2000-U). Minimum 3 images from each sample was analyzed using ImageJ to determine the number of live (green) and dead (red) cells . The cell viability was calculated by dividing the number of live cells by the total number of cells.

Phalloidin/DAPI staining was also performed to determine the role of hydrogel laden in various concentrations of PD-LAP on the cytoskeletal organization. The cell-seeded samples, at 1 and 3 days of culture, were fixed with 4% (v/v) paraformaldehyde (Sigma) solution and consequently were permeabilized using Triton X-100. To decrease the background staining, 2 wt% BSA in PBS was added to

the samples and was kept for 2h. After rinsing with PBS, the samples were incubated with rhodamine Phalloidin solution for 30 min. Consequently, 6-diamidine-2-phenyl indole dihydrochloride (DAPI, Sigma) solution was added to the samples. Following rinsing with PBS, the samples were imaged by a fluorescence microscope (Nikon TE 2000-U).

2.13. Statistical analysis

Statistical analysis was performed using one-way ANOVA, GraphPad Prism Software (V.6). P-value<0.05 was considered as a statistically significant.

3. Result and Discussion

3.1. Characterization of gelatin-based hydrogel

In this study, synthesis of blend composition of Gel-SH/GelMA with polydopamine functionalized Laponite® (PD-LAP) nanoplates and its application as an injectable and bioadhesive surgical sealants was evaluated. Due to the availability, biocompatibility, and non-immunogenicity gelatin has been widely used for various tissue engineering applications. Moreover, its derivatives of the collagen which is a component of extracellular matrix (ECM) and can mimic the ECM and provide the cell adhesion motifs such as RGD. Herein, we focused on two types of modifications comprising of methacrylation and thiolation processes. GelMA hydrogel was firstly prepared via a one-step methacrylation process (Supplementary Fig. S1A). FTIR spectra of gelatin and GelMA presented in Fig. S1B. The identified peaks in the spectra also exhibited in Supplementary Table S1. Compared to FTIR spectrum of gelatin, GelMA spectrum exhibited the characteristic peaks at 1272 cm^{-1} and 1548 cm^{-1}, related to the vibration of C-N bonds (related to amide I and II respectively), at 1631 cm^{-1} corresponded to the C=O bonds, at 2852 and 2922 cm^{-1} related to the C-H peaks and also at 3423 cm^{-1} referred to N-H bonds [33]. ^{1}H-NMR spectra of gelatin and GelMA also provided in Fig. S1C. Compared to the spectrum of gelatin, new signals were detected at 5.3 ppm and 5.5 ppm, relating to C=C bonds in the methacrylate (MA) groups. This result was similarly reported in previous researches and demonstrated the successful grafting of MA to gelatin backbone [34]. To determine the methacrylation degree, the ^{1}H-NMR spectrum of GelMA was quantified [35]. Our results revealed the methacrylation degree of about 87%, confirming the high methacrylation degree of gelatin [26].

The second functionalization process on gelatin was the thiolation process via a two-step amination and consequently thiolation procedure (Fig. 1A). Gelatin contains approximately 1000 µmol/g free carboxylate groups [6]. Upon the amination process, carboxylate groups of gelatin changed to primary amine groups. Then, the thiolation reaction was performed using 2-iminothilane to synthesize Gel-SH. ^{1}H-NMR results confirmed the successful grafting of thiol on the backbone of Gel-NH_2 (Fig. 1B). After the amination

process, the chemical signals at 1.24 ppm, 1.87 ppm and, 2.95 ppm, related to the different amine groups of gelatin structure increased. Also, at a one-step thiolation reaction, although the spectrum confirmed that the main amine peaks decreased, the thiol peak was not detected. It might be related to the low efficiency of thiolation reaction in the unmodified gelatin, owing to few amine groups presented in the gelatin structure. In the two-step thiolation reaction, the main amine peaks decreased and a new thiol peak appeared in the spectrum at 2.3 ppm, confirming the higher efficiency of two-step reaction compared to the one-step process. Moreover, another new peak at 3.2 ppm was visible (determined at higher magnification spectrum) which was related to new amine groups in the thiol reagent.

FTIR spectroscopy (Fig. 1C) also confirmed the thiolation process. Significant decrease in the intensity of OH and COOH peaks at around 3350 and 1640 cm^{-1} along with an increase in the intensity of NH_2 peak at around 3435 cm^{-1} in the spectrum of Gel-NH_2 confirmed the successful amination process[36]. In the second modification process, aminated groups converted to the thiol groups. FTIR spectrum of Gel-SH was consisted of a new peak at 2650 cm^{1} confirming the formation of new thiol groups in the structure of gelatin. Moreover, due to the presence of new amine groups in the structure of this component, the intensity of NH_2 group at around 3435 cm^{-1} was increased [37]. Furthermore, the number of thiol groups in the structure of hydrogel obtained from one and two-step thiolation reactions using the Ellman's protocol was calculated about 120±23 µmol/gr and 660±25 µmol/gr, respectively. The estimated thiol group on the surface of aminated gelatin (two-step thiolation process) was in the range and/or higher than those of previous researches [38], confirming the efficient amination and thiolation process.

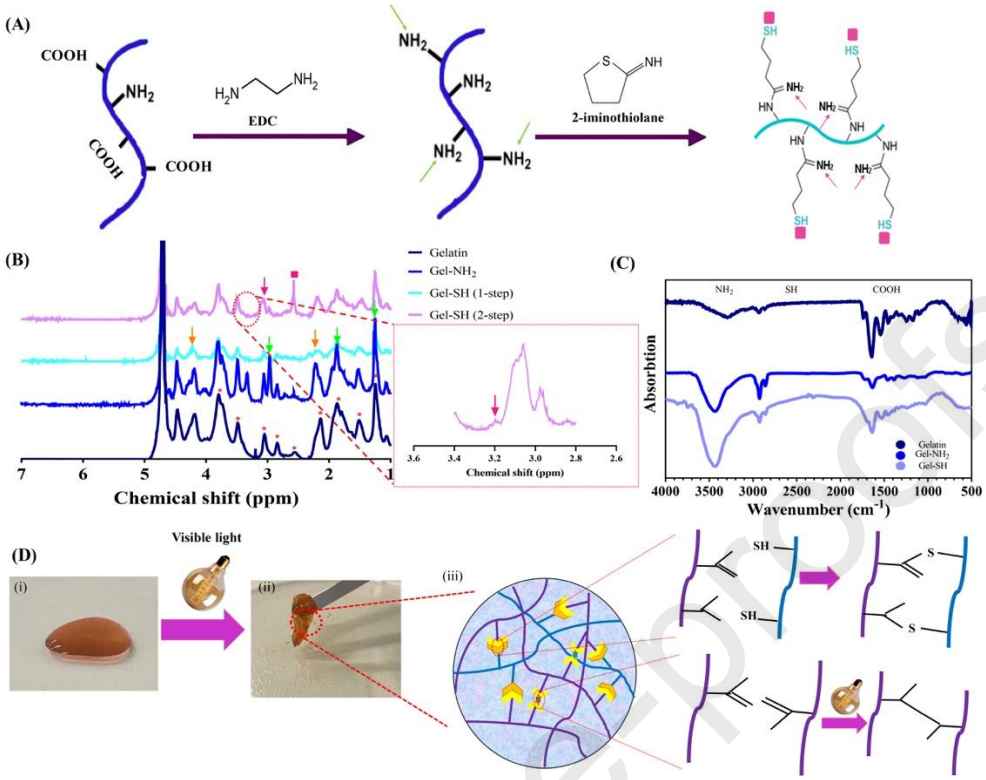

Fig. 1. Scheme and structural characterization of Gel-SH: (A) Scheme representation of the synthesize of Gel-NH_2 and Gel-SH. (B) ^{1}H-NMR spectra of gelatin, Gel-NH_2, Gel-SH (one-step) and Gel-SH (two-steps) confirming the chemical grafting of thiol on the gelatin structure. (C) FTIR spectra of gelatin, Gel-NH_2 and Gel-SH confirming the thiolation process. (D) The photographic images of gelatin based hydrogel, (i) before and (ii) after crosslinking with visible light. (iii) the scheme images of the gelatin based hydrogel containing two polymer chains of GelMA and Gel-SH interacted via thiol-methacrylate chemistry as well as photo-crosslinking process.

After mixing two pre-polymer solutions of GelMA and Gel-SH and consequently mixing them with photoinitiator and other components (Fig. 1D(i)), the hydrogels were crosslinked by 60 s exposure to the visible light (Fig. 1D(ii)). According to thiol-methacrylate chemistry, Michael addition interaction between thiol groups of Gel-SH and methacrylate groups of GelMA, may result in the formation of crosslinked hydrogels [13]. Moreover, after exposure to the visible light, the residual methacrylate groups of GelMA via radical polymerizations are crosslinked (Fig. 1D(iii)). The visible light crosslinking of GelMA established in the presence of Eosin Y (as photo-initiator), TEA as (co-initiator), and VC (co-monomer). During the visible-light exposure, Eosin Y molecules excited from the ground state into a triplet state that stimulate them to absorb the hydrogen atoms from TEA. Subsequently, the deprotonated radicals could initiate the vinyl bonds of VC, leading to chain polymerization, and subsequently hydrogel cross-linking [29]. UV-crosslinked GelMA has been extensively used for wound healing, and tissue engineering

applications [39]. However, the UV exposure has a detrimental effect on encapsulated cells and minor immune responses was reported in contact with UV cross-linked GelMA after subcutaneous implantation. This effect can be generated through the creation of reactive oxygen species (ROS) after exposure to UV light which can cause damaging the DNA of the encapsulated cells [40]. Eosin Y, a Food and Drug Administration (FDA)-approved photoinitiator has been recently applied in the FocalSeal®(lung sealant) [39] and TEA as a crosslinking agent in contact with various types of the cells such as fibroblasts [41] and human mesenchymal stem cells (hMSCs) has not shown any major toxicity; however the optimized concentration of TEA was determined less than 1.5 wt% [42]. Therefore, crosslinking system based on application of visible lights that can infiltrate within tissue and encapsulated cells at superior depths and lower energy, has shown significantly higher viability compared to UV light proving the system appropriate for minimally invasive applications.

*3.2. Characterization of polydopamine modified LAP nanosheets (*PD-LAP*)*

To provide strong interaction between LAP nanosheets and multi-crosslinked gelatin hydrogel, LAP nanoplates were successfully functionalized using polydopamine (Supplementary Fig. S2A). Consequently, PD-LAP with free catechol groups were produced (Fig. S2B). According to Fig. S2A, the color of the LAP solution (1mg/ml) changed from white to darkish gray after modification (PD-LAP solution), confirming the surface modification of LAP nanoplates. Zeta potential assay (Fig. S2C) also confirmed the difference between the surface electrostatic potential of LAP and PD-LAP. The formation of hydroxyl groups originated from PD structure on the surface of PD-LAP nanosheets resulted in a significant decrease in the zeta potential from -21.3±1.1 mV to -24.6±0.6 mV. Li et al.[43] revealed a similar result when graphene oxide nanoparticles coated with polydopamine. After incorporation of LAP nanoplates in the dopamine solution, the pH of solution enhanced to pH=8.5, leading to the self-polymerization of dopamine to PD [44]. Moreover, compared to the FT-IR spectrum of LAP (Fig. S2D), new peaks could be identified in the spectrum of PD-LAP at 1620, 1512 and 1297 cm^{-1} corresponded to C=C stretching vibration, N-H scissoring vibration and C-O stretching vibration of PD, respectively. Based on the PD polymerization reaction, the presence of N-H peak confirmed PD polymerization [45] where the new peaks were appeared in the lower wavelengths in Fig. S2D and Fig. 2D. Moreover, the presence of the phenol groups shown at 1051 cm^{-1} in the FTIR spectrum confirmed the polymerization of PDA [46]. Furthermore, in the XRD pattern of LAP nanosheets (Supplementary Fig. S2E) three characteristic peaks at $2\Theta=7.2^{\circ}$, 19.8 and 36.1° were visible which are belonged to (001), (02,11), and (005) reflection plans, respectively [20]. The $d_{(001)}$, $d_{(02,11)}$ and $d_{(005)}$ spacing were 1.22 nm, 0.22 nm and 0.248 nm, respectively. These d-spacing values were close to the d-values described in the literature [47]. After surface modification of LAP nanosheets with PD (PD-LAP), these characteristic peaks revealed a left-shift to $2\Theta=6.7^{\circ}$, 19.8° and 35.3°, respectively.

Therefore, the $d_{(001)}$ spacing, $d_{(02,11)}$ spacing and, $d_{(005)}$ spacing were estimated at 1.32 nm, 0.26 nm and 0.254 nm, respectively. Our results revealed that after in-situ polymerization of dopamine on the surface of LAP nanosheets, the d-spacing of LAP enlarged due to the intercalation of PD into the interlayer of LAP nanosheets [4]. Besides, dopamine polymerization caused a broad peak at around 2Θ=15-25° due to the amorphous structure of polydopamine [30]. These results confirmed the successful modification of LAP with polydopamine. It could be concluded that dopamine was oxidized by LAP nanosheets and PD intercalated between LAP layers, leading to an increase in the d-spacing of the LAP nanosheets. FE-SEM images of LAP and PD-LAP also presented in Fig. S2F. While both LAP and PD-LAP nanosheets were agglomerates of disk-shaped particles, PD modification process resulted in a minor change in the surface roughness of nanosheets. PD-LAP nanoplates revealed a rough surface due to the presence of PD on the surface of nanoparticles. Similarly, Mokhtari et al. [30] found that the coating of graphene oxide (GO) with polydopamine resulted in similar changes on the surface roughness of the nanosheets.

3.3. Characterization of nanocomposite hydrogels

In the next step, by changing the concentration of PD-LAP (0, 0.5, 1 and 2 wt%), a series of nanocomposite hydrogels were prepared. The gelation time is one of the most important properties of adhesive hydrogel for wound closure. Generally, fast gelation may lead to weaker hydrogels with low adhesive strength, as they do not have enough time for a strong network formation. Consequently, a gelation time of 5-60 s often required to provide appropriate mechanical and adhesive characteristics, depending on the applications[48]. Between our hydrogels, Gel-0%PD-LAP revealed the longest gelling time (about 55±5 s). Incorporation of PD-LAP nanosheets gradually reduced the gelling time to 50±3 s (0.5wt% PD-LAP), 45±5 s (1wt% PD-LAP), and 42±5 s (2wt% PD-LAP), confirming the effective role of these nanosheets to enhance the efficiency of gelation. The incorporation of PD-LAP nanosheets may provide a new interaction with the hydrogel network to stimulate hydrogel formation. Similarly, Liu et al. [49] also found that the curing time decreased from 1.8±0.1 min to 0.3±0.1 min with increasing LAP content up to 2 wt% in dopamine-modified four-armed poly(ethylene glycol) (PEG-D4) hydrogel.

Micrograph images of nanocomposite hydrogels obtained by SEM (Fig. 2A) revealed that all samples consisted of a highly porous structure with interconnected pores. However, the average pore diameter of hydrogels decreased from 39± 13 μm to 11±6 μm as PD-LAP content increased from 0 wt.% to 2 wt.% (Fig. 2B). Another effect of adding PD-LAP nanoplates to the hydrogel structure is decreasing the water absorption (results are provided in the section 3.4) which is the consequence of the reduced average pore size of hydrogels by increasing PD-LAP content. Li et al. [31] also demonstrated that the pore size of gelatin nanoparticles/poly(acrylamides) hydrogels decreased with increasing LAP content. Moreover, the disorganized structure of Gel-0%PD-LAP by addition of PD-LAP has changed to homogenous and uniform

porous structures. The organized microstructure of nanocomposite hydrogels at higher PD-LAP content might be due to the surface charge of the nanosheets, which improved their stability and homogeneity of the structure. Furthermore, EDS analysis (Fig. 2C) revealed the presence of the silicon from LAP nanosheets in the structure of the composite hydrogel. However, according to EDS-mapping analysis (Fig. 2D), while Si atoms were uniformly scattered on the whole surface of Gel-1%PD-LAP, the agglomerates of these atoms detected at Gel-2%PD-LAP. The higher magnification SEM image of Gel-2%PD-LAP also confirmed the agglomeration of PD-LAP nanoparticles in the walls of hydrogels (Fig. 2A).

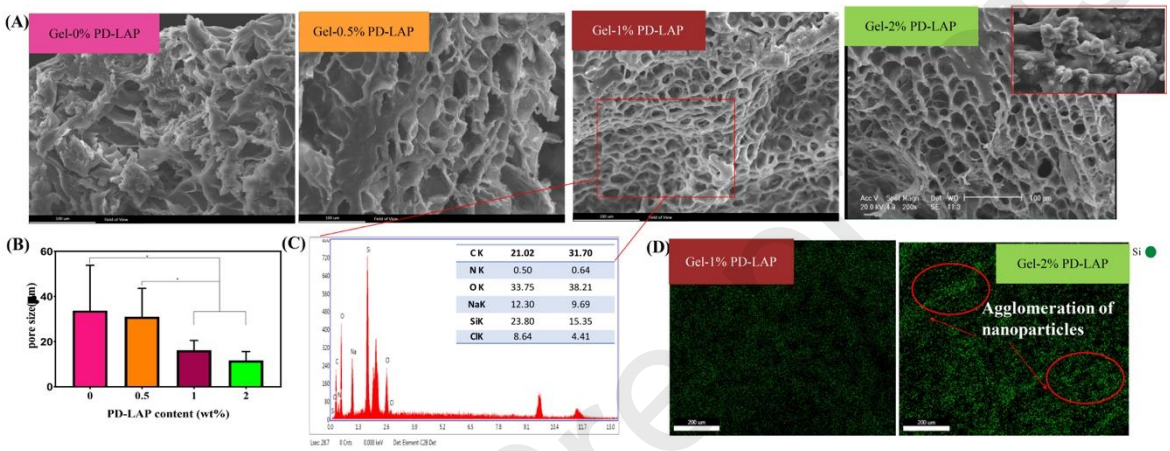

Fig. 2. Characterization of nanocomposite hydrogels: (A) SEM images of hydrogels compromising of different PD-LAP concentrations. (B) The average pore size and (C) the average pore area of nanocomposite hydrogels as a function of PD-LAP content, with the data shown as means ± SD (n = 3) (*: P<0.05). (D and E) EDS and mapping analysis of Gel-1%PD-LAP, confirming the presence of PD-LAP nanosheets and the uniform distribution of Si atom, respectively.

The Michael addition reaction between Gel-SH and GelMA, according to thiol-methacrylate chemistry, was confirmed by FT-IR spectroscopy (Fig. 3A). In comparison with GelMA spectrum, a decrease in the intensity of the acrylate groups at 1632 cm^{-1}, 1390 cm^{-1} and 808 cm^{1} in the mixture of GelMA/Gel-SH (hydrogel without any initiator) is related to the C=C bonds. Besides, the presence of a C-S bond at 1270 cm^{-1} and C=S at 1045 cm^{-1} confirmed the success of the Michael reaction [11]. After incorporation of photo-initiator in the structure of GelMA/Gel-SH (Gel-0%PD-LAP), according to Fig. 3B, new peaks were identified confirming the crosslinking between thiol and methacrylate groups. This spectrum consisted of new peaks at 1018, 1100 and 1273 cm^{-1} certified the presence of C=S, H-C-S and C-S in the structure due to the reaction of Sulfur in Gel-SH and Carbon in the GelMA structure, based on Michael reaction. Moreover, after incorporation of 2 wt%PD-LAP (Gel-2%PD-LAP sample), the intensity of C=O peaks of GelMA (at 1630 cm^{-1}) decreased and a new peak appeared at 1406 cm^{-1} related to the C-O peak. The

intensity of C-H bonds at 2970 cm^{-1} has increased which confirmed the formation of the new hydrogen bonding between catechol groups of PD-LAP and C=O bonds of GelMA [50]. Additionally, the shape, intensity, and position of the characteristic peak at 1018 cm^{-1}, after incorporation of PD-LAP, were changed which might be due to the physical crosslinking between C=S and Si-O-Si at this wavenumber. In conclusion, it can be explained that three different chemical interactions were responsible for hydrogel network formation. Photo-crosslinking of GelMA, Michael reaction between GelMA and Gel-SH and finally hydrogen bonding/physical interaction between PD-LAP and the gelatin-based structure.

3.4. In vitro swelling and degradation properties of nanocomposite hydrogels

The hydrophilic character of the hydrogels with high water content in their networks introduces them as suitable surgical glues and they are even able to absorb the wound exudate. Moreover, in wound-healing applications and sealants, the swelling ability is helpful for the diffusion of healing factors [18]. Here, the swelling ratio of the nanocomposite hydrogels after 24 h immersion in the PBS was calculated which confirmed the decreasing trend from 393±8% to 179±2%, when the PD-LAP content increased from 0 wt.% to 1 wt.%($P<0.05$) (Fig. 3C). However, the incorporation of more PD-LAP in the hydrogel network enhanced its swelling ratio. It needs to mention that the obtained swelling ratio of nanocomposite hydrogels was in the range of previous reported surgical adhesives [9]. The interaction between PD-LAP and hydrogel network could be a cause of prevention of water absorption affecting the swelling ratio. However, the enhanced swelling ratio of Gel-2%PD-LAP hydrogel might be related to the agglomeration of nanoparticles which resulted in the formation of weaker interactions between hydrogel matrix and PD-LAP nanoparticles. Similar findings were reported in other researches confirming the prominent role of LAP nanoparticles on the swelling behavior of Alginate-PVA [18] and poly(ethylene glycol) (PEG)-poly(trimethylene carbonate) (PTMC)[51].

The degradation rate of the nanocomposite hydrogels during 14 days of immersion in PBS was measured by monitoring the weight loss (Fig. 3D). The hydrogel with no nanoplates lost almost 72±4 % of the weight during the first 3 days and fully degraded after 14 days of incubation. However, the incorporation of PD-LAP increased the stability of the composite hydrogel where the degradation rate of Gel-0.5% PD-LAP and Gel-1% PD-LAP hydrogels significantly reduced to less than 40±4 % and 35±4%, respectively, after 14 days of incubation. It could be concluded that PD-LAP acted as an additional crosslinker in the structure and reduced the degradation rate of samples. This behavior was similarly reported for LAP incorporated PVA-Alginate hydrogels [18]. However, incorporation of 2 wt% PD-LAP in the hydrogel network significantly enhanced the weight loss upon 61±1%. It might be related to the increased swelling ratio of nanocomposite hydrogels and the agglomeration of nanoplates.

To determine the injectability of the hydrogels, the shear-thinning behavior of two compositions (Gel-0%PD-LAP and Gel-2%PD-LAP) was studied by applying various shear rates (0.01-200 1/s). In case of the pure hydrogel with no nanoplates (Gel-0%PD-LAP), the viscosity decreased from 10 Pa.s to 0.74 Pa.s, after applying the shear rate between 10^{-1} to 10^{2} confirming its shear-thinning behavior (Fig. 3E). Addition of PD-LAP nanoplates first increased the viscosity of Gel-2%PD-LAP pre-polymer to 18 Pa.s and applying shear rate from 10^{-1} to 10^{2} caused a decrease in the viscosity to 0.4 Pa.s. Formation of the non-covalent bonding between the PD-LAP and hydrogel network can be the reason of the increased viscosity. Moreover, polydopamine functionalization of nanoplates improved the interaction between PD-LAP and hydrogel structure. The shear-thinning behavior of Gel-2%PD-LAP hydrogel is presented in the supplementary Video S1. Xavier et al. [52] also studied the rheological behavior of GelMA-LAP nanocomposite hydrogel and similarly found that the incorporation of LAP in the GelMA polymer induced the shear-thinning properties in the hydrogel. Moreover, Lokhande et al. [53] reported the reduced viscosity from 10 Pa.s to 0.5 Pa.s, for nanosilicates/kappa-carrageenan hydrogels, when the shear rate increased from 10^{-1} to 10^{2}. Mokhtari et al. [30] also demonstrated that the presence of PD coated graphene oxide (GOPD) improved the shear-thinning and self-healing properties of the kappa-carrageenan hydrogel due to the incorporation of new electrostatic bonds between catechol groups in GOPD and the matrix.

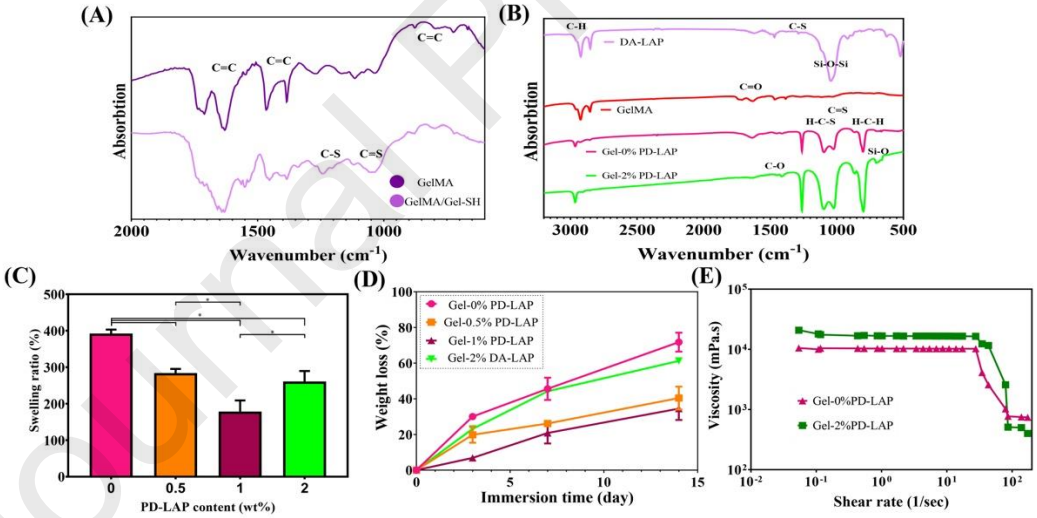

Fig. 3. Characterization of nanocomposite hydrogels: FTIR spectra of (A) GelMA and GelMA-Gel-SH and (B) Gel-0%PD-LAP and Gel-2%PD-LAP nanocomposite hydrogels, along with GelMA and PD-LAP. (C) Swelling ratio and (D) degradation profile of nanocomposite hydrogels as a function of PD-LAP concentration, with the data shown as means ± SD (n = 3) (*: P<0.05). (E) Viscosity changes of pre-polymers of Gel-0%PD-LAP and Gel-2%PD-LAP as function of shear rate.

3.5. Mechanical properties of nanocomposite hydrogels

The compressive stress-strain graphs of nanocomposite hydrogels consisting of different PD-LAP contents after applying 60% strain is presented in Fig. 4A. All curves obeyed a similar trend, including two distinct regions. The first region, known as the toe area, was related to the initial deformation of samples. The second region (knee region) was correlated to the resistance of nanocomposite networks against the mechanical forces [54]. The strength of the samples after 60% strain was calculated and presented in Fig 4B. Results demonstrated that incorporation of 1 wt% PD-LAP significantly enhanced the compressive strength (2.8 times) from 54±2 kPa to 153±7 kPa ($P<0.05$). However, incorporation of more PD-LAP noticeably reduced the compressive strength of nanocomposite hydrogels owing to the agglomerates of nanoparticles. Xavier et al. [52] reported the compressive strength of GelMA-LAP nanosheets in 60% strain was less than 40 kPa. This improvement in the compressive strength of the present nanocomposite hydrogel was related to the increase in the crosslinking density of hydrogel networks and functionalization of the LAP nanoplates. Covalent bonding between Gel-SH and GelMA in addition to the incorporation of PD-LAP improved the mechanical strength by emerging stronger bonding between PD-LAP and the hydrogel network.

The tensile test was also performed on the nanocomposite hydrogels and elastic modulus (Fig. 4C), tensile strength (Fig. 4D), toughness (Fig. 4E) and elongation (Fig. 4F) were obtained. The calculated elastic moduli was in the range of 6-31 kPa, which is in the range of the reported values for surgery sealants [4] and tensile strength was in the range of 20-80 kPa for various concentrations of PD-LAP. Furthermore, the extensibility of nanocomposite hydrogels by increasing PD-LAP content upon 1 wt.% was improved for ~1.8-fold higher (from 35±2% to 63±5%) and then in higher concentration was reduced. Results indicated that the highest toughness of nanocomposite hydrogels was obtained at Gel-1%PD-LAP, due to the strong chemical crosslinking, which enhanced both tensile strength and elongation of samples. In the developed composite hydrogel, seems that Michael reaction has played the main role in improvement of the mechanical strength where it formed a new covalent bond between thiol groups of Gel-SH and methacrylate groups of GelMA. Besides that, the photo-crosslinking of methacrylate groups on GelMA structure and homogenous distribution of PD-LAP nanoparticles in the nanocomposite hydrogels provided an homogenous crosslinked network between nanosheets and hydrogel network, which able to dissipate stress during deformation [55]. However, incorporation of 2 wt% PD-LAP in hydrogel structure has shown a detrimental effect on mechanical properties of nanocomposite hydrogels which was due to the inhomogeneous distribution and agglomeration of PD-LAP nanoplates.

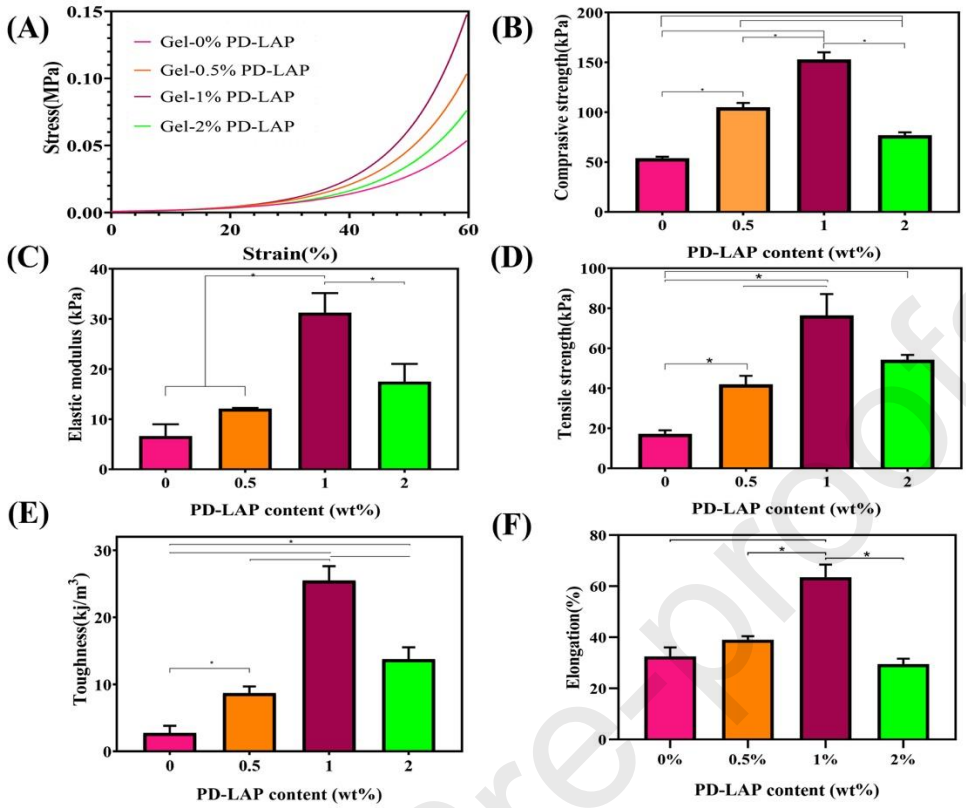

Fig. 4. Mechanical properties of nanocomposite hydrogels: (A) Compressive stress-strain curves. (B) Compressive strength, (C) elastic modulus, (D) tensile strength, (E) toughness and (F) elongation changes as a function of PD-LAP, with the data shown as means ± SD (n = 3) (*: P<0.05).

An adhesive sealant in contact with wound is facing the dynamic loading such as cyclic stretching or compression; therefore, in this study we have tested the stability of the adhesive hydrogel under cyclic forces. In this case, the compressive cyclic loading-unloading was applied and stress-strain curves of nanocomposite hydrogels under five sequential cycles were obtained (Fig. 5A). Based on these curves, toughness (amount of absorbed energy) and dissipated energy (amount of energy which absorbed and dissipated) (Fig. 5B) during the cyclic test were estimated. Moreover, the recovery of the hydrogels (the ability of hydrogels to recover the absorbed energy in different cycles) was assessed by comparing the toughness of hydrogels in each cycle to the 1st cycle (Fig. 5C). According to the compressive loading-unloading curves of Gel-0%PD-LAP, the strength of hydrogels with increasing the number of compressive cycles reduced. However, the initial strain for each cycle increased with a low slope. Therefore, the toughness of Gel-0%PD-LAP (Fig. 5B) decreased from 1.3±0.04 kJ/m^3 at the first cycle to 0.8±0.05 kJ/m^3 after the fifth cycle. Moreover, the denser hysteresis loop demonstrated a decrease in the dissipated energy

of Gel-0%PD-LAP hydrogel (Fig. 5B). Interestingly, the hydrogel with no nanosheets (Gel-0%PD-LAP) showed stability after the 2nd cycle and curves were more similar, which can be related to the interactions between Gel-SH and GelMA. In continue, the effect of PD-LAP content on the loading-unloading behavior of nanocomposite hydrogels was tested, where incorporation of 0.5 wt.% PD-LAP showed enhancement of the strength and toughness of the hydrogel at approximately all cycles without disrupting the steady-state in the last three cycles. It means that the presence of PD-LAP in the hydrogel networks enhanced the stability of the structure in continues cycles which was an important parameter in the dynamic loading. By increasing the amount of PD-LAP upon 1 wt%, a significant increase in the strength and toughness was observed in all cycles especially in the 1st cycle (2.64 folds) ($P<0.05$). Mehrali et al. [37] similarly investigated the cyclic properties of pectin methacrylate (PEMA)/ Gel-SH hydrogel and showed that the maximum total energy dissipation of the hydrogel was about 1.35±0.5 kJ/m^3 with the maximum strength of 9±3 kPa. In comparison with our current data, incorporation of PD-LAP to Gel-SH/GelMA hydrogel resulted in an increase in the strength and toughness to 22±2 kPa and 2.8±0.3 kJ/m^3, respectively. The recovery percentage in each cycle was also determined based on the changes in comparison with the toughness of the first cycle. According to Fig. 5C, although the stability of all hydrogels in the last three cycles was confirmed, incorporation of 1 wt% PD-LAP, improved the stability of hydrogel from the 2nd cycle. By increasing the amounts of PD-LAP upon 2 wt%, the ability of hydrogels in the compressive strength, toughness and absorbing and dissipating energy were sharply decreased which could be related to the agglomeration of PD-LAP and consequently weak interaction between nanosheets and polymeric chains.

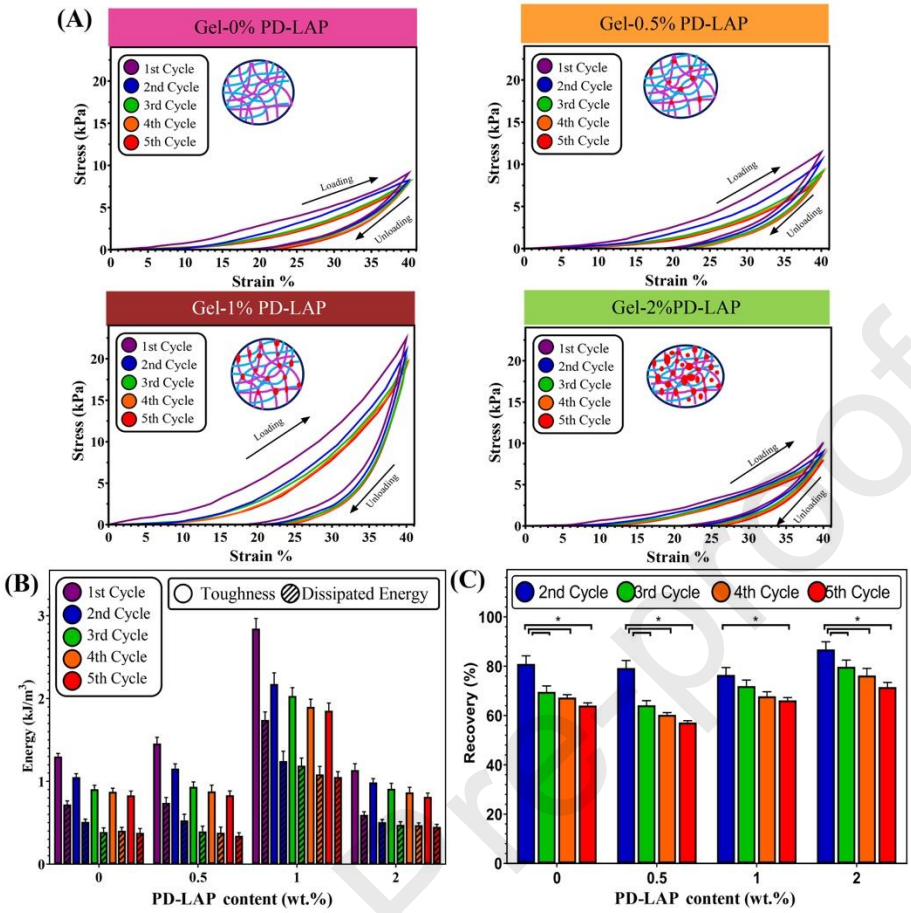

Fig. 5. The compressive cyclic properties of nanocomposite hydrogel: A) Compressive loading-unloading curves and the anticipated structure of Gel-0% PD-LAP, Gel-0.5%PD-LAP, Gel-1%PD-LAP and Gel-2%PD-LAP hydrogels. (B) Toughness and dissipated energy of nanocomposite hydrogels as a function of PD-LAP concentration. (C) Recovery percentage in different cycles as a function of PD-LAP concentration, with the data shown as means ± SD (n = 3) (*: P<0.05).

3.6. Tissue adhesive strength of nanocomposite hydrogels

One of the crucial drawbacks in the adhesive sealants is their weak adhesive strength in the wet condition. According to the representative images in Fig. 6A, the nanocomposite hydrogels (Gel-2%PD-LAP) adhered tightly to the skin and tolerated various types of stresses (Fig. 6A(i-iv)). Moreover, Fig. 6A(v) showed that this nanocomposite hydrogel was able to adhere to skin and detach simply without initiating any damage, therefore, the adhesive strength of samples significantly was improved due to the presence of PD-LAP in the structure. Noticeably, the adhesive strength (Fig. 6B) was significantly increased from 68.7±1 kPa (at Gel-0%PD-LAP) to 116.1±34 kPa (at Gel-2%PD-LAP) (P<0.05). This strength was significantly superior

to that of commercial sealants such as Evicel™, Coseal™ surgical sealants and Fibrin glues [29]. Elvin et al.[56] also reported the similar tissue adhesion strength (>100 kPa) for porcine gelatin, bovine gelatin, and bovine fibrinogen. The improved adhesion strength can be due to the interactions between thiol groups and methacrylate groups, and the strong binding affinity of catechol groups to various nucleophiles in the hydrogel network such as amines and thiol groups. Enhanced crosslinking density resulted from these interactions resulted in higher cohesive strength of the hydrogel structure. Different interactions between the nanocomposite hydrogels and skin are schematically described in Fig. 6C. Moreover, the catechol-containing amino acids presenting in the structure of PD could anchor to peptides and proteins on the tissue surface, providing a hypothetical mechanism for tissue adhesion of these nanocomposites. This is the predominant mechanism for nearly all adhesives and sealants containing polydopamine [57]. Catechol is a unique adhesive molecule that can bond to both organic and inorganic surfaces with covalent interactions. Oxidation of catechol groups forms a highly reactive Quinone. Quinone acts as an intermolecular covalent crosslinker and increases the adhesive ability by increasing reactions with nucleophile molecules (NH_2) on the biological substrates. Han et al. [4] demonstrated that increasing the catechol groups in the structure of the hydrogel enhanced its ability to adhere to the surfaces. Also, Liu et al.[49] demonstrated that the presence of 2 wt% PD modified LAP nanosheets increased the adhesive strength of PEGDA hydrogel up to 7.5±2 kPa. Moreover, Ninan et al.[58] used MAP (mussel adhesive proteins) and crosslinked them with V^{+6} and reported the adhesive strength of 462± 46 kPa confirming the unique adhesive properties of MAP, DOPA and dopamine. Besides, the modification of the gelatin backbone chain with amine and thiol groups improved the penetration of hydrogel to the sheep skin tissue (Fig. 6C). It could be concluded that the Gel-PD-LAP nanocomposite hydrogels can be considered as a potential candidate for surgical sealants, specifically for internal surgeries.

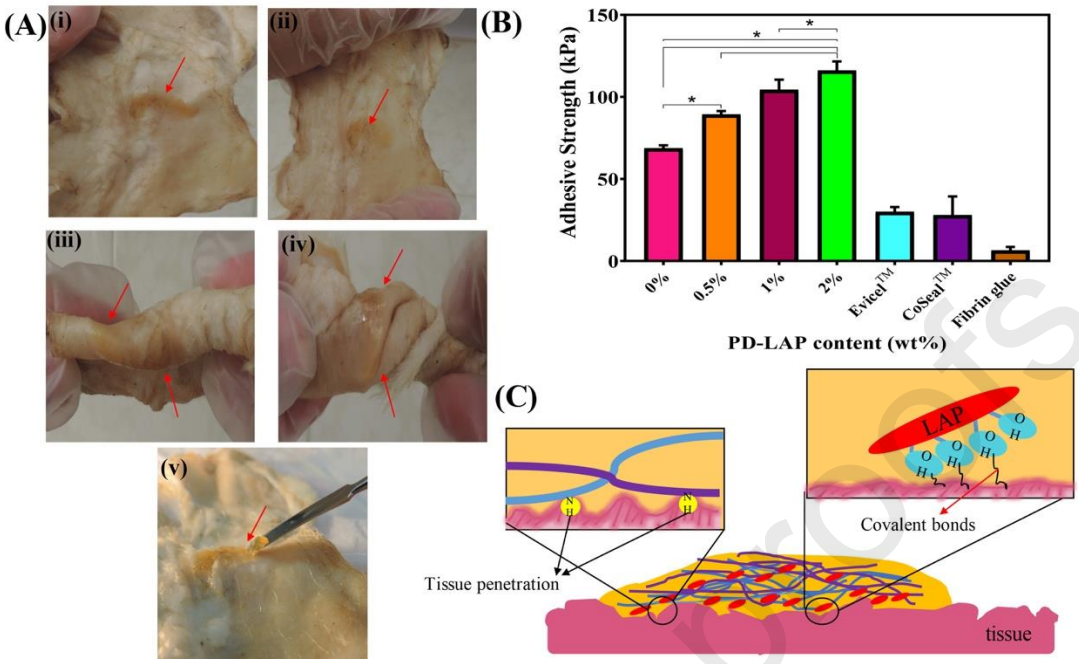

Fig. 6. Adhesive properties of nanocomposite hydrogels: (A) Photographs of Gel-1%PD-LAP hydrogel adhered to sheepskin under (i) normal condition and under (ii) tensile, (iii) torsion, and (iv) twist deformation, confirming the high adhesion strength. (v) The nanocomposite hydrogels removed completely from the skin, demonstrating their highly cohesive strength. (B) Adhesive strength changes of nanocomposite hydrogels as a function of PD-LAP content. The adhesion strength of hydrogels was compared with the results of three commercial glues, with the data shown as means ± SD (n = 3) (*: $P<0.05$). (C) Schematic representation of tissue penetration and new covalent bonds between tissue and nanocomposite hydrogels.

3.7. Protein absorption of nanocomposite hydrogels:

The amount of BSA adsorption on the surface of the sealants is the first step in thrombosis formation [18]; Therefore, we evaluated the effect of the PD-LAP on absorption of BSA and the results are summarized in Fig. 7A. It was shown that BSA absorption was increased 1.3-fold higher from 3.9±0.3 mg/g to 5.16±0.23 mg/g, when PD-LAP content enhanced from 0 wt.% to 2 wt.% ($P<0.05$). This is due to the changes in surface charge of Gel-SH and PD-LAP in the structure of nanocomposite hydrogels, which resulted in increased adsorption of BSA [59].

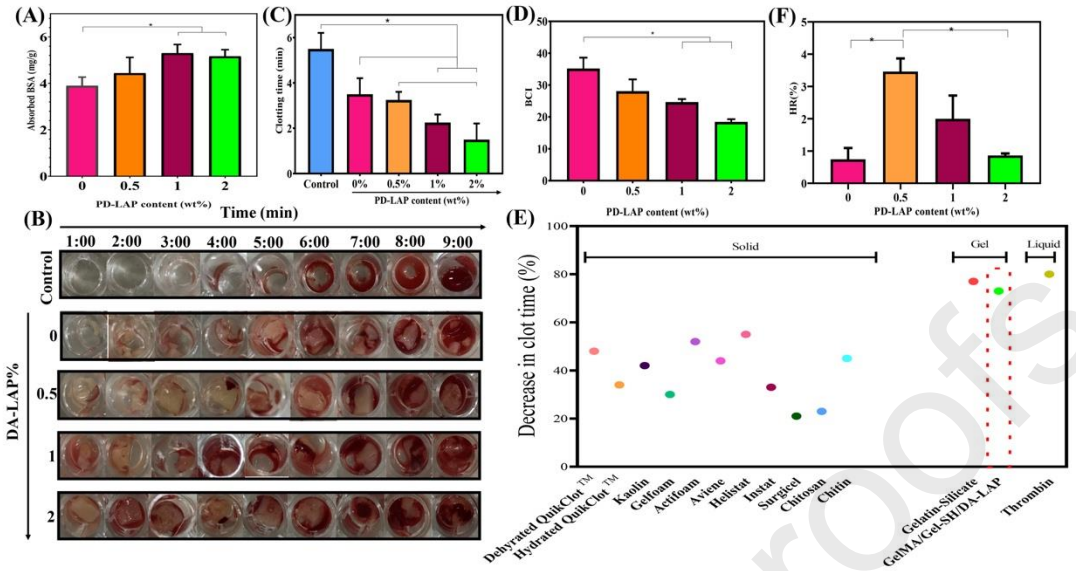

Fig. 7. Blood compatibility of hydrogels: (A) BSA absorption on the nanocomposite hydrogels as a function of PD-LAP concentration. (B), (C) Effect of PD-LAP concentration on the blood clotting time. (D) BCI index of nanocomposite hydrogels as a function of PD-LAP concentration. (F) Comparison of clotting time for Gel-PD-LAP hydrogels with commercial glues and previous studies[7]. (E) HR% of nanocomposite hydrogels as a function of PD-LAP concentration, with the data shown as means ± SD (n = 3) (*: P<0.05)

3.8. Blood compatibility evaluation of nanocomposite hydrogels

The hemostatic ability of nanocomposite hydrogels was estimated by examining the clotting time of blood in contact with samples (Fig. 7B). According to Fig. 7C, the blood clotting time of control sample was determined about 5.5±0.5 min. This time was in agreement with previous reports [7, 60] In contact with Gel-0%PD-LAP hydrogel, the blood clotting time was reduced to 3.5±0.5 min (Fig. 7B). The hygroscopic structure of gelatin and its tamponade ability could result in the absorption of fluid components of blood without the stimulation of clot formation [7]. The reduced blood clotting time in this condition, compared to control also might be due to the negative charge of Gel-SH. However, it was not significantly different from blood clotting time on the control (P>0.05). Increasing the PD-LAP content upon 2 wt.% (P<0.05) resulted in shorter blood clotting time to about 1.5±0.5 min (Fig. 7B). Another parameter related to the blood clotting ability of samples is the blood clotting index (BCI, the UV-absorbance of blood clots in contact with samples) (Fig. 7D). Higher blood clotting ability caused higher stability of the clot and lower flowing behavior which led to a decrease in the BCI index[61]. By increasing the content of PD-LAP concentration from 0 wt.% to 2 wt.% (P<0.05), the BCI of the nanocomposite hydrogels was decreased 1.9-fold from 35±2 to 18±1. It could be due to the intense negative charge of LAP nanoplates which was greatly

improved after modification with PD (supplementary Fig. S2C). Previous studies also demonstrated a significant decrease in the blood clotting time after the incorporation of negatively charged materials [62]. Interaction of blood with the negatively charged surface can facilitate platelet aggregation and activate the intrinsic pathway of blood clotting. The XII factor primarily activated in contact with samples leading to the thrombosis formation. Consequently, the clot formed due to the polymerization of fibrinogen monomers into fibrin [18]. So, increasing the negative charges on the surface and increased protein adsorption promote the blood clotting ability of the sealant. The comparison of blood clotting time measured in the nanocomposite hydrogels, developed in our study, and different kinds of hemostatic products (solid, gel and liquid) [7] is summarized in Fig. 7E. It can be seen that gels and especially hydrogels with varying amounts of LAP revealed the shortest blood clotting time. Moreover, this improvement in blood clotting was similar to the reported data for hemostats based on thrombin [63]. Here, our hydrogel with decrease of clotting time more than 72% showed significant improvement comparing to other sealants.

To evaluate the blood compatibility of nanocomposite hydrogels, Hemolysis assay was also performed. Generally, HR of all nanocomposite hydrogels was less than the level of 5%, showing these hydrogels were non-hemolytic [64]. However, it was found that the HR value of various samples was different, depending on the PD-LAP content. For instance, HR percentages of nanocomposite hydrogels significantly enhanced 4.4-fold from 0.8±0.3% to 3.5±0.3% when PD-LAP concentration was reached to 0.5 wt.% which might be due to the negative surface charges of PD-LAP nanoparticles. Golafshan et al.[18] reported similar results. However, incorporation of more PD-LAP nanoplates decreased the hemolysis ratio of nanocomposite hydrogels; which was due to the functionalized surface of nanoplates with PD as well as the agglomeration of PD-LAP at Gel-2%PD-LAP. It has been reported before that polydopamine had effect on reduction of the hemolytic activity of biomaterials [65]. For instance, in the study reported by Yang et al. [59], PD coating decreased the HR% of the 316L samples. In conclusion, the effective role of incorporated PD-LAP in hydrogel structure as a potential sealant was observed where it resulted in decreased blood clotting time, reduced hemolysis ratio and increased blood compatibility.

3.9. Cell Culture

To study the cytocompatibility of nanocomposite hydrogels with different PD-LAP concentrations, L929 cells were seeded on the samples and cell proliferation was evaluated using MTT assay (Fig. 8A). Higher cell viability was measured after 5 days of culture on various hydrogels confirming the cytocompatibility of samples. Moreover, cell survival enhanced by increasing PD-LAP content. For instance, after 5 days of culture, in contact with Gel-2%PD-LAP hydrogel, the higher viability (105.7±7.5 (%control)) was measured which was 1.2 times greater than on the Gel-0%PD-LAP (82.3±3.6 (%control)). A similar result was reported for other nanocomposite hydrogels such as LAP-PEG [66] and LAP/PVA-alginate [18] in

contact with different types of cells. The viability of fibroblast cells cultured on the hydrogels was also measured using live/dead kit after 1 and 5 days of culture. According to Fig. 8B and C, the cell viability on various hydrogels was greater than 85% and cell viability enhanced with increasing culture time, showing that all samples were not cytotoxic. Moreover, the cell viability enhanced with increasing PD-LAP content. For instance, after 3 days of culture, the viability of fibroblast cells enhanced from 90.5±0.5% (at Gel-0%PD-LAP) to 97.5±0.75% (Gel-2%PD-LAP) ($P<0.05$). Incorporation of LAP nanosheets not only improved the mechanical properties and blood clotting ability of the hydrogels, but also showed high cell viability, and proliferation. It can be related to the structure of LAP and the release of inorganic ions such as Mg^{+2}, Na^{+}, $Si(OH)_4$ and Li^{+} from LAP nanoplates in contact with the physiological environment [18]. LAP nanoplates could be dissolved in the aqueous environment at all pH values, depending on the LAP concentration. According to the pH value of the environment, either H^{+} or OH^{-} ions could dissociate from the LAP edges leading to the negative or positive charge, respectively. Consequently, released ions, and variation of the pH value of the solution can affect the LAP stability. In the presence of H^{+} ions, LAP nanoparticles could degrade leading to leaching of magnesium (Mg^{+2}) and lithium (Li^{+}) ions, based on the following reaction[67]:

$$Na_{0.7}Si_8Mg_{5.5}Li_{0.3}O_{20}(OH)_4+12H^{+}+8H_2O \rightarrow 0.7Na^{+}+8Si(OH)_4+5.3Mg^{2+}+0.4Li^{+}$$

These mineral ions, especially Mg^{2+}, could noticeably influence the cell function [68]. For instance, they acted as a stimulator for cell proliferation and increased cell survival. Moreover, modification of LAP nanosheets with polydopamine improved cell proliferation because of expanding the catechol groups of polydopamine [69].

In the next step, we evaluated the cytoskeletal organization of cells adhered to the nanocomposite hydrogels after 3 days of culture. According to Fig. 8D, the hydrogel composition affected the cell morphology, and density. The stained nucleus was counted to estimate the number of cells assessed after 1 and 3 days of culture (Fig. 8E). It confirmed that the nanocomposite hydrogels supported the adhesion and proliferation of fibroblasts. After one day of culture, the number of adhered cells on the hydrogels significantly enhanced with increasing PD-LAP concentration ($P<0.05$) which can be the effect of the polydopamine coating as well as modulation of the mechanical properties of the hydrogels, affecting the biomechanic of the material to a favorable stiffness for cell adhesion [70]. Moreover, the number of cells spread on the samples was also increased after 3 days for samples containing 1 and 2 wt% PD-LAP. Cells completely covered the surface of Gel-2%PD-LAP hydrogel and started to expand their cytoskeleton and form connections. The relation of the biochemical signals released from the substrates, their bio-mechanic and effects on cytoskeleton of cells has been previously reported by Gaharwar et al. [54]. They showed that incorporation of different amounts of LAP in the PEG hydrogel significantly increased the cell attachment on the hydrogel

surface. In another study [71], they suggested that incorporation of LAP in the PEG hydrogels enhanced the protein absorbance and consequently increased the attachment of cells on the sample surfaces. Con et al. [4] also reported the positive effect of PD coating in the polyacrylamide-clay hydrogel on the enhanced cell adhesion. Higher cell adhesion was also reported in polydopamine incorporated hydrogels [30] and polydopamine coated metals [72] due to the higher protein adsorption.

Generally, to provide an effective adhesive hydrogel for surgical sealants, various properties including mechanical properties, swelling ratio, blood compatibility, clotting time and biocompatibility should be optimized. In this study, nanocomposite hydrogels, specifically consisting of 1 and 2% PD-LAP were cytocompatible and could promote attachment, spreading and proliferation of fibroblasts. Various elastic modulus of this material was advantageous to adjust the properties based on the target tissue that require an adhesive sealant. For instance, lung sealants need to have an elastic modulus in the range of 5-30 kPa to support lung tissue inflation and deflation [73] and both Gel-1% PD-LAP and Gel-2%PD-LAP hydrogels revealed a similar range of elastic modulus. However, the weak dynamic behavior, low elongation and high swelling ratio of Gel-2%PD-LAP are not appropriate for highly stressed tissues like lung and arteries. [73],[74]. Therefore, elasticity, acceptable clotting time similar to the regular surgical sealants made Gel-1% PD-LAP, a better candidate for such application [48].

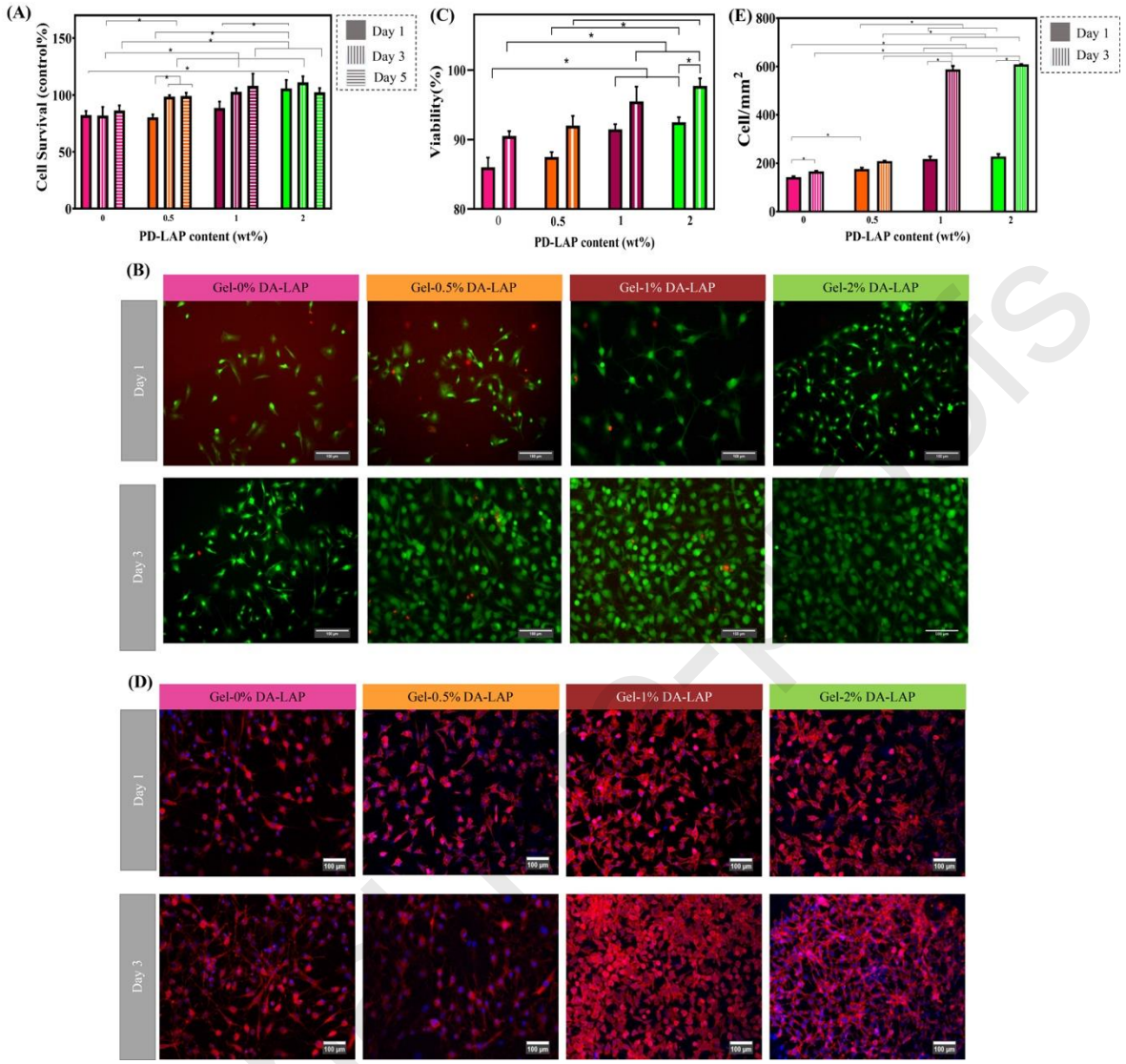

Fig. 8. Cytocompatibility of nanocomposite hydrogels: (A) Effect of PD-LAP concentration on the cell viability using MTT assay at different culture times (1, 3 and 5 days). The absorbance of samples was normalized against TCP. (B) The illustrative fluorescence images of live/dead assay at days 1 and 3 of culture. The live and dead cells were stained by Calcein AM(green) and EthDII (red), respectively. (C) The cell viability calculated based on number of live cells. (D) Representative fluorescence images of the stained cells with DAPI (blue) and rhodamine-phalloidin (red). (E) The cell proliferation determined according to DAPI staining, with the data shown as means ± SD (n = 3) (*: $P<0.05$).

Conclusion

In this study, we developed a visible-light crosslinked nanocomposite hydrogel based on thiolated gelatin (Gel-SH)/gelatin methacrylate (GelMA) compromising of various amounts of polydopamine-functionalized LAP (PD-LAP) for surgical sealants. The variation of the physical properties of nanocomposite hydrogels such as pore size, mechanics, swelling behavior and degradation rate, for different PD-LAP concentration, was carefully analyzed . Noticeably, the incorporation of 1 wt%PD-LAP significantly enhanced the tensile strength (4.4 times), toughness (9.3 times), and elongation (2 times) of Gel-SH/GelMA hydrogel and promoted its dynamic properties in the cyclic compressive test. Compared to other GelMA, and thiolated gelatin-based hydrogels [52], our nanocomposite hydrogels revealed significantly higher mechanical strength. Besides, PD-LAP nanoparticles improved the tissue adhesive strength, blood clotting ability, cytocompatibility, and blood compatibility of Gel-SH/GelMA hydrogel. Moreover, the nanocomposite hydrogel significantly decreased the blood clotting time (1.5±0.5 min), compared to the commercial adhesives such as *Helistat ™and Avitene ™hemostatic sealant [7]*. Different from other gelatin-based bioadhesive sealants [75], this work studied the effects of PD-LAP on the blood clotting, biodegradation, swelling ratio, mechanical properties, tissue adhesive strength, and cytocompatibility of gelatin-based hydrogels. The combination of Michael addition reaction, photocrosslinking, and covalent interactions between various components have resulted in significant improvement in the properties of gelatin-based bioadhesive hydrogels. Further evaluations are still in progress. Overall, the results demonstrated that this nanocomposite hydrogel at the optimal concentration of PD-LAP (1 wt%) could be a promising hydrogel for hemostatic surgical sealants.

Reference

[1] V. Bhagat, M.L. Becker, Degradable Adhesives for Surgery and Tissue Engineering, Biomacromolecules 18(10) (2017) 3009-3039.
[2] N. Annabi, A. Tamayol, S.R. Shin, A.M. Ghaemmaghami, N.A. Peppas, A. Khademhosseini, Surgical materials: Current challenges and nano-enabled solutions, Nano Today 9(5) (2014) 574-589.
[3] P. Sergeant, R. Kocharian, B. Patel, M. Pfefferkorn, J. Matonick, Needle-to-suture ratio, as well as suture material, impacts needle-hole bleeding in vascular anastomoses, Interactive Cardiovascular and Thoracic Surgery 22(6) (2016) 813-816.
[4] N. Annabi, Y.N. Zhang, A. Assmann, E.S. Sani, G. Cheng, A.D. Lassaletta, A. Vegh, B. Dehghani, G.U. Ruiz-Esparza, X. Wang, S. Gangadharan, A.S. Weiss, A. Khademhosseini, Engineering a highly elastic human protein-based sealant for surgical applications, Science Translational Medicine 9(410) (2017) eaai7466.
[5] P. Aramwit, N. Jaichawa, J. Ratanavaraporn, T. Srichana, A comparative study of type A and type B gelatin nanoparticles as the controlled release carriers for different model compounds, Materials Express 5(3) (2015) 241-248.
[6] S. Duggan, The synthesis and characterisation of mucoadhesive polymeric systems using synthetic and natural polymers, Waterford Institute of Technology, 2015.
[7] A.K. Gaharwar, R.K. Avery, A. Assmann, A. Paul, G.H. McKinley, A. Khademhosseini, B.D. Olsen, Shear-thinning nanocomposite hydrogels for the treatment of hemorrhage., ACS nano 8(10) (2014) 9833-9842.

[8] F.L. Nicolas, C.H. Gagnieu, Denatured thiolated collagen: II. Cross-linking by oxidation, Biomaterials 18(11) (1997) 815-821.
[9] X.Z. Shu, S. Ahmad, Y. Liu, G.D. Prestwich, F. Palumbo, G.D. Prestwich, Disulfide-crosslinked hyaluronan-gelatin hydrogel films: a covalent mimic of the extracellular matrix for in vitro cell growth, Biomaterials 24(21) (2003) 3825-3834.
[10] Y. Xiao, L.A. Reis, N. Feric, E.J. Knee, J. Gu, S. Cao, C. Laschinger, C. Londono, Diabetic wound regeneration using peptide-modified hydrogels to target re-epithelialization, Proceedings of the National Academy of Sciences 113(40) (2016) E5792-E5801.
[11] T. Wang, J. Wang, X. He, Z. Cao, D. Xu, F. Gao, J. Zhong, L. Shen, An Ambient Curable Coating Material Based on the Michael Addition Reaction of Acetoacetylated Castor Oil and Multifunctional Acrylate, Coatings 9(1) (2019) 37.
[12] W.M. Li, D.M. Liu, S.Y. Chen, L. Li, C. Lu, L. Wang, M. Chen, J. White, X. Hao, K.M. McLean, H. Chen, T.C. Hughes, Gelatin-based photocurable hydrogels for corneal wound repair, ACS applied materials & interfaces 10(16) (2018) 13283-13292.
[13] J.A. Kornfield, A. Fu, K. Gwon, M. Kim, G. Tae, J.A. Kornfield, Visible-light-initiated thiol–acrylate photopolymerization of heparin-based hydrogels, Biomacromolecules 16(2) (2015) 497-506.
[14] D.y. Teng, Z.m. Wu, X.g. Zhang, Y.x. Wang, C. Zheng, Z. Wang, C.x. Li, Synthesis and characterization of in situ cross-linked hydrogel based on self-assembly of thiol-modified chitosan with PEG diacrylate using Michael type addition, Polymer 51(3) (2010) 639-646.
[15] S. Faghihi, M. Gheysour, A. Karimi, R. Salarian, Fabrication and mechanical characterization of graphene oxide-reinforced poly (acrylic acid)/gelatin composite hydrogels, Journal of Applied Physics 115(8) (2014) 083513.
[16] Y. Chen, B. Bilgen, R.A. Pareta, A.J. Myles, H. Fenniri, D.M. Ciombor, R.K. Aaron, T.J. Webster, Self-Assembled Rosette Nanotube/Hydrogel Composites for Cartilage Tissue Engineering, Tissue Engineering Part C: Methods 16(6) (2010) 1233-1243.
[17] Y. Gao, Y. Han, M. Cui, H.L. Tey, L. Wang, C. Xu, ZnO nanoparticles as an antimicrobial tissue adhesive for skin wound closure, Journal of Materials Chemistry B 5(23) (2017) 4535-4541.
[18] N. Golafshan, R. Rezahasani, M.T. Esfahani, M. Kharaziha, S.N. Khorasani, Nanohybrid hydrogels of laponite: PVA-Alginate as a potential wound healing material, Carbohydrate polymers 176 (2017) 392-401.
[19] S. Yixue, C. Bin, G. Yuan, W. Chaoxi, Z. Lingmin, C. Peng, W. Xiaoying, T. Shunqing, Modification of agarose with carboxylation and grafting dopamine for promotion of its cell-adhesiveness, Carbohydrate Polymers 92(2) (2013) 2245-2251.
[20] M. Roozbahani, M. Kharaziha, R. Emadi, pH sensitive dexamethasone encapsulated laponite nanoplatelets: Release mechanism and cytotoxicity, International Journal of Pharmaceutics 518(1-2) (2017) 312-319.
[21] M. Atrian, M. Kharaziha, R. Emadi, F. Alihosseini, Silk-Laponite® fibrous membranes for bone tissue engineering, Applied Clay Science 174 (2019) 90-99.
[22] M. Roozbahani, M. Kharaziha, Dexamethasone loaded Laponite®/porous calcium phosphate cement for treatment of bone defects, Biomedical Materials 14(5) (2019) 55008-55008.
[23] J.I. Dawson, R.O.C. Oreffo, Clay: New opportunities for tissue regeneration and biomaterial design, Advanced Materials 25(30) (2013) 4069-4086.
[24] S. Malekkhaiat Häffner, L. Nyström, K.L. Browning, H. Mörck Nielsen, A.A. Strömstedt, M.J. Van Der Plas, A. Schmidtchen, M. Malmsten, Interaction of Laponite with Membrane Components—Consequences for Bacterial Aggregation and Infection Confinement, ACS Applied Materials & Interfaces 11(17) (2019) 15389-15400.

[25] L. Han, X. Lu, K. Liu, K. Wang, L. Fang, L.-T. Weng, H. Zhang, Y. Tang, F. Ren, C. Zhao, Mussel-inspired adhesive and tough hydrogel based on nanoclay confined dopamine polymerization, ACS nano 11(3) (2017) 2561-2574.
[26] J.W. Nichol, S.T. Koshy, H. Bae, C.M. Hwang, S. Yamanlar, A. Khademhosseini, Cell-laden microengineered gelatin methacrylate hydrogels, Biomaterials 31(21) (2010) 5536-5544.
[27] S.R. Popuri, A. Harris-Logie, K.H. Lino, E.I. Cadogan, C.H. Lee, Evaluation of antibacterial activity and characterization of synthesized biodegradable copolymers., Polymer-Plastics Technology and Engineering 53(15) (2014) 1625-1635.
[28] (!!! INVALID CITATION !!! [7, 8]).
[29] S. Tavakoli, M. Kharaziha, A. Kermanpur, H. Mokhtari, Sprayable and injectable visible-light Kappa-carrageenan hydrogel for in-situ soft tissue engineering, International Journal of Biological Macromolecules 138 (2019) 590-601.
[30] H. Mokhtari, M. Kharaziha, F. Karimzadeh, S. Tavakoli, An injectable mechanically robust hydrogel of Kappa-carrageenan-dopamine functionalized graphene oxide for promoting cell growth, Carbohydrate polymers 214 (2019) 234-249.
[31] C. Li, C. Mu, W. Lin, T. Ngai, Gelatin Effects on the Physicochemical and Hemocompatible Properties of Gelatin/PAAm/Laponite Nanocomposite Hydrogels, ACS Applied Materials & Interfaces 7(33) (2015) 18732-18741.
[32] M.F. Shih, M.D. Shau, M.Y. Chang, S.K. Chiou, J.K. Chang, J.Y. Cherng, Platelet adsorption and hemolytic properties of liquid crystal/composite polymers, International Journal of Pharmaceutics 327(1-2) (2006) 117-125.
[33] (!!! INVALID CITATION !!! [32, 33]).
[34] L. Zhou, G. Tan, Y. Tan, H. Wang, J. Liao, C. Ning, Biomimetic mineralization of anionic gelatin hydrogels: effect of degree of methacrylation, Rsc Advances 4(42) (2014) 21997-22008.
[35] W.T. Brinkman, K. Nagapudi, B.S. Thomas, E.L. Chaikof, Photo-cross-linking of type I collagen gels in the presence of smooth muscle cells: mechanical properties, cell viability, and function., Biomacromolecules 5(4) (2003) 890-895.
[36] C. Tengroth, U. Gasslander, F.O. Andersson, S.P. Jacobsson, Cross-linking of gelatin capsules with formaldehyde and other aldehydes: An FTIR spectroscopy study, Pharmaceutical Development and Technology 10(3) (2005) 405-412.
[37] M. Mehrali, A. Thakur, F.B. Kadumudi, M.K. Pierchala, J.A.V. Cordova, M.A. Shahbazi, M. Mehrali, C.P. Pennisi, G. Orive, A.K. Gaharwar, A. Dolatshahi-Pirouz, Pectin Methacrylate (PEMA) and Gelatin-Based Hydrogels for Cell Delivery: Converting Waste Materials into Biomaterials, ACS Applied Materials and Interfaces 11(13) (2019) 12283-12297.
[38] (!!! INVALID CITATION !!! [9, 38]).
[39] I. Noshadi, S. Hong, K.E. Sullivan, E.S. Sani, R. Portillo-Lara, A. Tamayol, S.R. Shin, A.E. Gao, W.L. Stoppel, L.D. Black III, A. Khademhosseini, In vitro and in vivo analysis of visible light crosslinkable gelatin methacryloyl (GelMA) hydrogels. , Biomaterials science 5(10) (2017) 2093-2105.
[40] S.J. Bryant, C.R. Nuttelman, K.S. Anseth, Cytocompatibility of UV and visible light photoinitiating systems on cultured NIH/3T3 fibroblasts in vitro. , Journal of Biomaterials Science, Polymer Edition 11(5) (2000) 439-457.
[41] M. Bikram, C. Fouletier-Dilling, J.A. Hipp, F. Gannon, A.R. Davis, E.A. Olmsted-Davis, J.L. West, Endochondral bone formation from hydrogel carriers loaded with BMP2-transduced cells. , Ann Biomed Eng 35(5) (2007) 796-807.
[42] C.S. Bahney, T.J. Lujan, C.W. Hsu, M. Bottlang, J.L. West, B. Johnstone, Visible light photoinitiation of mesenchymal stem cell-laden bioresponsive hydrogels. , European cells & materials 22 (2011) 43.

[43] G. Li, Y. Liang, C. Xu, H. Sun, L. Tao, Y. Wei, X. Wang, Polydopamine reinforced hemostasis of a graphene oxide sponge via enhanced platelet stimulation, Colloids and Surfaces B: Biointerfaces 174 (2019) 35-41.
[44] L. Han, X. Lu, K. Liu, K. Wang, L. Fang, L.-T. Weng, H. Zhang, Y. Tang, F. Ren, C. Zhao, Mussel-Inspired Adhesive and Tough Hydrogel Based on Nanoclay Con fi ned Dopamine Polymerization, ACS nano 11(3) (2017) 2561-2574.
[45] (!!! INVALID CITATION !!! [29, 45, 47, 48]).
[46] (!!! INVALID CITATION !!! [29, 45]).
[47] S. Boudjemaa, B. Djellouli, Characterization of Organomontmorillonite (Organo-Mmt) and Study of Its Effects upon The Formation of Poly (Methyl Methacrylate)/Organo-Mmt Nanocomposites Prepared by in situ Solution Polymerisation, Russ. J. Appl. Chem. 87 (2014) 1464-1473.
[48] C. Ghobril, M.W. Grinstaff, The chemistry and engineering of polymeric hydrogel adhesives for wound closure: a tutorial., Chemical Society Reviews 44(7) (2015) 1820-1835.
[49] Y. Liu, H. Meng, S. Konst, R. Sarmiento, R. Rajachar, B.P. Lee, Injectable dopamine-modified poly(ethylene glycol) nanocomposite hydrogel with enhanced adhesive property and bioactivity, ACS Applied Materials and Interfaces 6(19) (2014) 16982-16992.
[50] Y. Liu, Y. Sui, C. Liu, C. Liu, M. Wu, B. Li, Y. Li, A physically crosslinked polydopamine/nanocellulose hydrogel as potential versatile vehicles for drug delivery and wound healing, Carbohydrate polymers 188 (2018) 27-36.
[51] S. Sharifi, S.B. Blanquer, T.G. van Kooten, D.W. Grijpma, Biodegradable nanocomposite hydrogel structures with enhanced mechanical properties prepared by photo-crosslinking solutions of poly (trimethylene carbonate)–poly (ethylene glycol)–poly (trimethylene carbonate) macromonomers and nanoclay particles., Acta biomaterialia 8(12) (2012) 4233-4243.
[52] J.R. Xavier, T. Thakur, P. Desai, M.K. Jaiswal, N. Sears, E. Cosgriff-Hernandez, R. Kaunas, A.K. Gaharwar, Bioactive nanoengineered hydrogels for bone tissue engineering: A growth-factor-free approach, ACS Nano 9(3) (2015) 3109-3118.
[53] G. Lokhande, J.K. Carrow, T. Thakur, J.R. Xavier, M. Parani, K.J. Bayless, A.K. Gaharwar, Nanoengineered injectable hydrogels for wound healing application, Acta biomaterialia 70 (2018) 35-47.
[54] A.K. Gaharwar, R.K. Avery, A. Assmann, A. Paul, G.H. McKinley, A. Khademhosseini, B.D. Olsen, C.P. Rivera, C.-J. Wu, G. Schmidt, Transparent, elastomeric and tough hydrogels from poly (ethylene glycol) and silicate nanoparticles, Acta biomaterialia 7(12) (2011) 4139-4148.
[55] C.J. Wu, A.K. Gaharwar, P.J. Schexnailder, G. Schmidt, Development of biomedical polymer-silicate nanocomposites: a materials science perspective, Materials Express 3(5) (2010) 2986-3005.
[56] C.M. Elvin, T. Vuocolo, A.G. Brownlee, L. Sando, M.G. Huson, N.E. Liyou, P.R. Stockwell, R.E. Lyons, M. Kim, G.A. Edwards, G. Johnson, A highly elastic tissue sealant based on photopolymerised gelatin, Biomaterials 31(32) (2010) 8323-8331.
[57] (!!! INVALID CITATION !!! [2, 59]).
[58] L. Ninan, R.L. Stroshine, J.J. Wilker, R. Shi, Adhesive strength and curing rate of marine mussel protein extracts on porcine small intestinal submucosa. , Acta biomaterialia 3(5) (2007) 687-694.
[59] Z. Yang, Q. Tu, Y. Zhu, R. Luo, X. Li, Y. Xie, M.F. Maitz, J. Wang, N. Huang, Mussel-inspired coating of polydopamine directs endothelial and smooth muscle cell fate for re-endothelialization of vascular devices, Advanced Healthcare Materials 1(5) (2012) 548-559.
[60] S.E. Baker, A.M. Sawvel, N. Zheng, G.D. Stucky, Controlling Bioprocesses with Inorganic Surfaces: Layered Clay Hemostatic Agents. , Chem. Mater. 19 (2007) 4390–4392.
[61] M.F. Shih, M.D. Shau, M.Y. Chang, S.K. Chiou, J.K. Chang, J.Y. Cherng, Platelet adsorption and hemolytic properties of liquid crystal/composite polymers. , International journal of pharmaceutics 327(1-2) (2006) 117-125.
[62] (!!! INVALID CITATION !!! [7, 18, 62]).

[63] W.R. Wagner, J.M. Pachence, J. Ristich, P.C. Johnson, Comparative in Vitro Analysis of Topical Hemostatic Agents. , J. Surg. Res 66 (2009) 100–108.
[64] C. Mu, F. Liu, Q. Cheng, H. Li, B. Wu, G. Zhang, W. Lin, Collagen cryogel cross-linked by dialdehyde starch, Macromolecular Materials and Engineering 295(2) (2010) 100-107.
[65] (!!! INVALID CITATION !!! [61, 66, 67]).
[66] (!!! INVALID CITATION !!! [56, 68]).
[67] S. Jatav, Y.M. Joshi, Chemical stability of Laponite in aqueous media, Applied Clay Science 97 (2014) 72-77.
[68] J.K. Carrow, L.M. Cross, R.W. Reese, M.K. Jaiswal, C.A. Gregory, R. Kaunas, I. Singh, A.K. Gaharwar, Widespread changes in transcriptome profile of human mesenchymal stem cells induced by two-dimensional nanosilicates., Proceedings of the National Academy of Sciences 115(17) (2018) E3905-E3913.
[69] (!!! INVALID CITATION !!! [29, 71]).
[70] (!!! INVALID CITATION !!! [4, 7, 72]).
[71] A.K. Gaharwar, C.P. Rivera, C.J. Wu, G. Schmidt, Transparent, elastomeric and tough hydrogels from poly(ethylene glycol) and silicate nanoparticles, Acta Biomaterialia 7(12) (2011) 4139-4148.
[72] M. Liu, J. Zhou, Y. Yang, M. Zheng, J. Yang, J. Tan, Surface modification of zirconia with polydopamine to enhance fibroblast response and decrease bacterial activity in vitro: a potential technique for soft tissue engineering applications, Colloids and Surfaces B: Biointerfaces 136 (2015) 74-83.
[73] N. Annabi, Y.N. Zhang, A. Assmann, E.S. Sani, G. Cheng, A.D. Lassaletta, A. Vegh, B. Dehghani, G.U. Ruiz-Esparza, X. Wang, S. Gangadharan, Engineering a highly elastic human protein–based sealant for surgical applications., Science translational medicine 9(410) (2017) eaai7466.
[74] A. Assmann, A. Vegh, M. Ghasemi-Rad, S. Bagherifard, G. Cheng, E.S. Sani, G.U. Ruiz-Esparza, I. Noshadi, A.D. Lassaletta, S. Gangadharan, A. Tamayol, A highly adhesive and naturally derived sealant. , Biomaterials 140 (2017) 115-127.
[75] (!!! INVALID CITATION !!! [7, 54]).

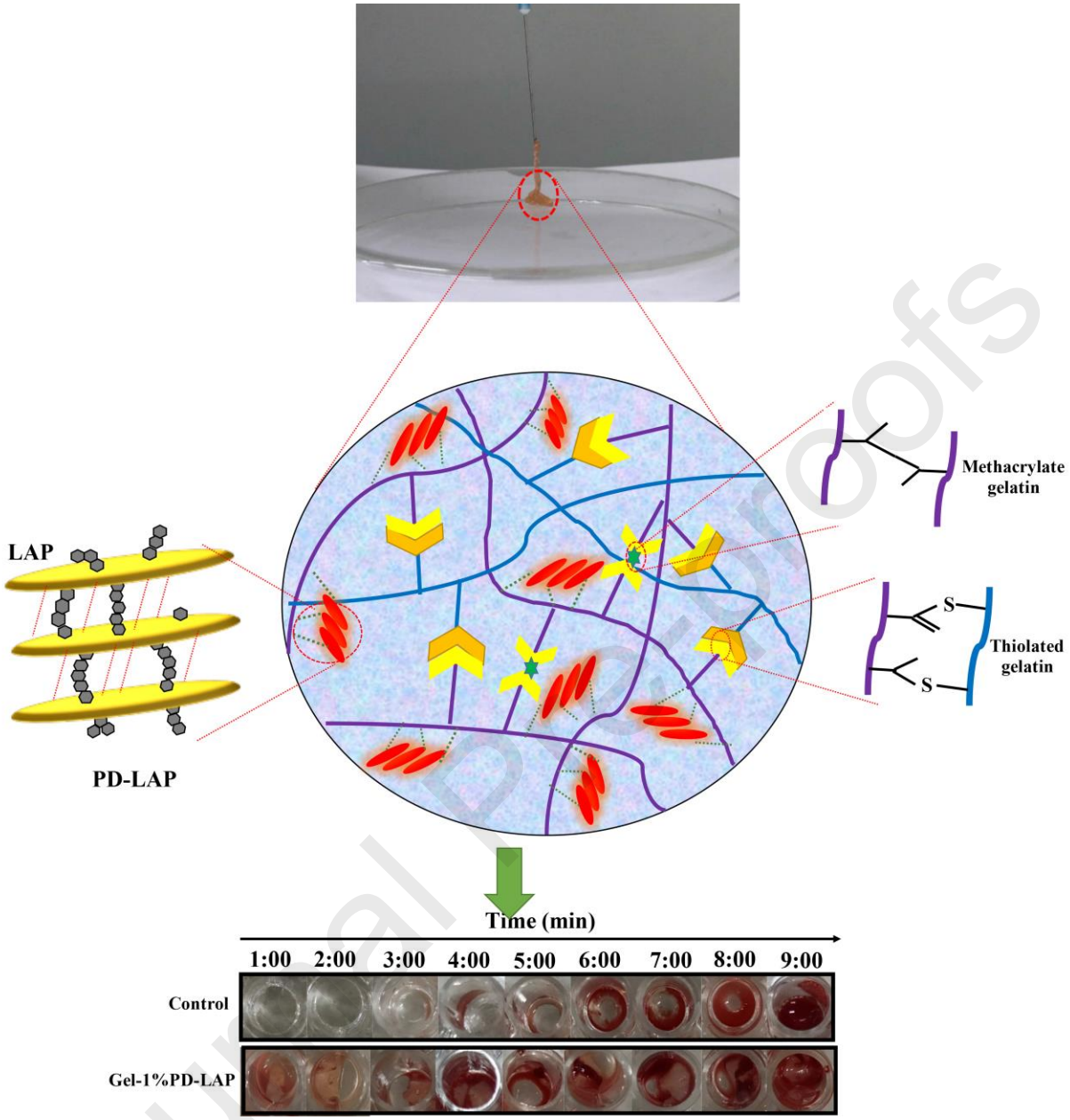

Declaration of interests

☒ The authors declare that they have no known competing financial interests or personal relationships that could have appeared to influence the work reported in this paper.

☐The authors declare the following financial interests/personal relationships which may be considered as potential competing interests:

Author Contribution Statement

N.R.: Investigation, Writing the original work, Visualization, Formal analysis

M.K: Supervision, Project administration, Funding acquisition, Visualization, Conceptualization

R. E: Supervision, Funding acquisition

A. Z: Methodology, Validation

H.M: Formal analysis, Software

S.S: Writing and Software